The Hong Kong Polytechnic University
Department of Mechanical Engineering

A Study of Perforated Panels for Sound Absorption

by

Law Lok Yin, Peter

A thesis submitted in partial fulfilment of the requirements for the Degree of Master Philosophy

July, 2003

CERTIFICATE OF ORIGINALITY

I hereby declare that this thesis is my own work and that, to the best of my knowledge and belief, it reproduces no material previously published or written nor material which has been accepted for the award of any other degree or diploma, except where due acknowledgement has been made in the text.

_____ , _____(Signed)

Law Lok Yin, Peter (Name of student)

Abstract of thesis entitled 'A Study of Perforated Panels for Sound Absorption' submitted by Law Lok Yin, Peter for the degree of Master of Philosophy at The Hong Kong Polytechnic University.

Abstract

A general analytical model for the evaluation of sound attenuation and absorption coefficient of common sound absorbers has been established. Compared with common theoretical predictions, this model is more general because it includes the sound attenuation by interference effect above the sound absorbers, and the absorption coefficient of the absorbers. The study uses various kinds of sound absorbers as testing specimens, including fibrous absorbers, micro-perforated panel absorbers, perforated panel absorbers, and mixed construction (fibrous materials covered with micro-perforated panel or perforated panel) absorbers. Outdoor sound measurement is conducted to obtain the sound attenuation by interference effect above the sound absorbers, the impedance tube and reverberation testing method is used to determine the normal and average absorption coefficient of the absorbers respectively.

The first part of our study is to introduce the basic theory of predicting the acoustic impedance and sound attenuation above the sound absorption materials. Outdoor sound measurements are conducted in order to determine the surface impedance of the fibrous absorbers and to measure the sound attenuation above the absorbers. Based on the outdoor sound propagation theory, a model is proposed for predicting sound absorption coefficient in spherical wave condition. In the common theoretical model for sound absorber, they assume infinite distance between the sound source and receiver. The proposed model can be used for both cases of infinite and finite distance between the sound source and receiver, and therefore it can provide more accurate prediction. The absorption coefficient of the absorbers depend on the range of receiver and the position of source and receiver.

In the second part of the thesis, the classical Maa's theory is firstly reviewed. The unproved formula of oblique acoustic impedance of micro-perforated panel absorber as

proposed by Maa is validated by the author using numerical fitting method by outdoor sound propagation theory. The impedance model of fibrous materials covered with micro-perforated panel is introduced. Outdoor sound measurement is conducted to consolidate the impedance and realize the sound attenuation by interference effect above the absorbers. Furthermore, a proposed theory based on the outdoor sound propagation theory and the classical Dah-You Maa theory is presented for the sound absorption performance of the micro-perforated panel absorber. Compared to Maa's theory, the model is more general because it includes the sound attenuation and the absorption coefficient of the micro-perforated panel absorber. The theoretical prediction has good agreement with the experimental results. Moreover, the absorption coefficient of fibrous materials covered with micro-perforated panel are predictable based on the proposed theory.

In the final section of the thesis, a theory for predicting the surface impedance of perforated facings on sound absorption materials is established. Boundary element method (BEM), the existing approximate BEM and 3-dimensional approximate BEM is used to verify the impedance model of the absorbers based on the proposed model. Good agreements between the predicted results and BEM results have been obtained. Moreover, an equivalent electrical circuit approach (EECA) is briefly reviewed in order to verify the normal and average absorption coefficient in spherical wave condition of sound absorbers. This is a more general analytical model of predicting sound attenuation by interference effect and absorption coefficient of micro-perforated panel absorber as well as perforated panel absorber.

Acknowledgement

I would like to express my sincere gratitude to my supervisors, Dr. W.O.Wong and Dr. K.M.Li, for their continuous encouragement, supervision and precious advice. I would also like to express my appreciation to them for their valuable suggestions and encouragement.

I am indebted to the colleagues of the acoustic group for their hospitality and technical assistance during the set up and the measurement. I wish to thank The Hong Kong Polytechnic University for the financial support. I would also like to give special thanks to the staff of Armstrong-Hiltion Limied for their superb proofreading.

Table of Contents

List of Figures

CHAPTER 2

CHAPTER 3

CHAPTER 1

Introduction

1.1 Background of the Research Work

In recent years, there have been many theoretical and experimental acoustical characterisations of different types of sound absorbers. Undoubtedly, the characterisation of sound absorbers is a significant theme in noise control engineering. The sound attenuation and the absorption coefficient are two important factors in clarifying the absorption performance of sound absorption materials. However, many researchers have only considered one aspect during investigation. Thus, the present study will establish a general analytical model that is used to determine the absorption performance of different types of sound absorbers (fibrous materials absorbers, micro-perforated panel absorbers, perforated panel absorbers). The common measurement techniques to obtain the absorption coefficient and sound attenuation are, respectively, impedance tube or reverberation room measurement and maximum length sequence (MLS) analysis.

1.1.1 Fibrous materials absorbers

In general, fibrous materials consist of glass or rock wool, have high acoustic absorption, and are fireproof. Therefore, they are widely used as sound absorption materials in the noise control engineering. However, the structure of fibrous materials is complicated and analysis is not easily performed. Zwikker and Kosten and Biot[1] proposed a theoretical model for fibrous materials five decades ago. Recently, Attenborough[2], Allard et al., Stinson and Champoux, and others have modified the method to make it more applicable. Moreover, Wilson developed a relaxation model

that has few parameters and can be applied with reasonable accuracy to any fibrous material. Delany and Bazley[3] proposed an empirical formula to estimate the characteristic impedance and propagation coefficient of fibrous materials. This formula is widely used to describe sound propagation in fibrous material, but it is not suitable for very low and very high frequencies.

1.1.2 Micro-perforated panel absorbers

In 1974, Dr. Dah-Yau Maa[4] found that if the diameter of the holes on a metal plate is reduced to between 0.1 and 1 mm, then it can provide high acoustic resistance and low acoustic mass reactance for the sound absorbers without additional fibrous materials. Thus, micro-perforated panel (MPP) absorbers were developed in the late 1960s without the use of any fibrous material. The absorption performance of the MPP absorber is only dependent on the design and the parameters of the micro-perforated panel[5].

Recent research has shown that when the holes of MPP absorbers are reduced to below 1 mm, the MPP acoustic resistance increases tremendously. Moreover, the ratio of acoustic resistance to acoustic mass reactance increases strictly. If the ratio of acoustic resistance to acoustic mass reactance is high, then the MPP absorber forms an efficient sound absorbing construction without the use of any fibrous material. In general, the perforation ratio indicates that the ratio of the total area of the pores to that of the panel is low to obtain good absorption performance[6]. Moreover, the panel can be made of any material, such as cardboard, plastic or sheet metal. The absorption performance of using cardboard for micro-perforated panel absorber should be similar in using metal. It is because the absorption performance of micro-perforated panel absorber is mainly depended on diameter of the hole, spacing between the holes and the

air cavity. However, if micro-perforated panel absorber is made of cardboard, it will be damaged very easily than metal and low durability.

After investigating a single layer of MPP absorber, Maa went on to find that double layer MPP absorbers[7] give a wide frequency band efficiency purpose for adverse circumstances in reverberation or noise control. In general, double resonators are also useful to extend the absorption to very low frequencies. The absorption may extend to low frequencies and high frequencies, especially when a random incidence is considered[8,9]. For mid frequencies, the absorption performance of the double layer MPP absorber is improved due to the resonance within the two air cavities. Thus, it is more useful to use the double layer MPP absorber for industrial applications.

In general, the absorption performance of MPP absorber is mainly on low and medium frequencies. For indoor application, people often use the absorbers for controlling reverberation time within certain room volume to optimum design at 500 or 1000Hz. In fact, MPP absorber is very popular and suitable for indoor application because it is non-fibrous, clean and flexible for interior acoustic design. Recently, there have been many measurements of MPP absorber performance using impedance tubes and reverberation rooms. Moreover, experimental measurements of mixed MPP construction (MPP + fibrous materials) absorbers have been carried out to obtain absorption coefficients. The purpose was to compare the relationship between the normal and random incidence of sound waves. During the experimental testing, researchers found that if the construction of the MPP absorber is uncovered along the boundary, then the absorption performance is best. In addition, the absorption coefficient of random incidence has been established using Maa's experimental studies. However, no theoretical prediction of the absorption coefficient of mixed MPP construction has been reported in the literature. Experimental results show that the absorption performance of the mixed MPP absorbers is better than the MPP absorber

alone at lower frequencies. The reason for this is that the acoustic resistance of fibrous materials is increased by covering them with MPP. However, the absorption performance at higher frequencies is reduced because the surface area of the fibrous material has been partially covered.

1.1.3 Membrane absorbers

Alternatively, metal membranes can be used as absorbing elements. Recent studies have found that the sound absorption of membrane absorbers is good at low and medium frequencies. These studies refer to the sound absorption coefficient and acoustic impedance for normal incidence of the sound waves. It is shown that the behaviour of the absorbing element is mainly determined by a combination of Helmholtz resonance and plate resonance. When properly dimensioned, a good absorption performance is achieved at low and medium frequencies. These properties make the element appropriate for special requirements in industrial applications. The complicated structure of the membrane absorber makes it clear that its acoustic behaviour depends on a number of construction parameters, and the material properties. Thus, the design of an optimised absorber for a particular application is a complicated task. Recent research[10] has included many analytical and experimental studies of the influence of various construction parameters on the membrane absorbers for the normal incidence of sound waves.

1.1.4 Micro-perforated panel membrane absorbers

Theories for both membrane absorbers and microperforated panel absorbers have been well developed. However, no theory gives us information on combinations such as glass-fibre textiles or a micro-perforated membranes mounted over an air cavity. Actually, some research papers have presented a theoretical method for predicting the

absorption of such a structure. The basic idea of the theory is to regard an open weave textile or a micro-perforated membrane as a parallel connection of the membrane and apertures. The prediction for the normal incidence and random incidence of sound waves has shown very good agreement with the experimental measurements in recent studies. This kind of structure can demonstrate that the absorption performance is very high. The micro-perforated membrane absorber would have notable advantages in practice because it is lightweight, inexpensive, and does not use any fibrous materials.

1.1.5 Perforated panel absorbers

Perforated panel absorbers are commonly used in architectural and industrial noise control engineering. In recent years, a new theoretical model for predicting the sound absorption of perforated absorber systems has been presented. The system with a perforated panel consists of an arbitrary combination of fibrous and air layers backed by a rigid wall. This model includes the effect of the diffraction phenomenon caused by impedance discontinuities of the boundary surface, which was disregarded in the past studies. In fact, perforated panel absorbers have been widely used in architectural acoustics and the control of noise control problems. Such absorbers have many complex phenomena that affect their performance. This kind of analytical model gives a good prediction for sound absorption characteristics over the whole frequency range and is useful for practical applications.

Actually, the materials used in perforated panel absorbers are very efficient for sound absorption at high frequencies, but are comparatively poor at low frequencies. Ordinary perforated panels with holes of several millimetres or centimetres have low acoustic resistance, which disallows good sound absorbing construction without the use additional fibrous materials such as fiberglass or mineral wool. Therefore, the best way to use this sort of panel is for protective facings only. In the early 1980s Soerman

published his research results on duct silencing using perforated panels. However, his silencers were constructed using panels with large holes (1.6–3.2 mm diameter). Such large hole silencers have low and narrow band insertion loss[11]. Therefore, the absorption efficiency of this kind of silencer is low.

1.1.6 *Outdoor sound prediction*

According to traditional methodology, the attenuation of a sound field over a surface or ground can be determined by outdoor sound propagation theory. In fact, the sound field due to reflection on a surface is dependent on the location of the receiver relative to the source, and on the properties of the reflecting plane. Moreover, surface acoustic impedance is used to quantify the effect of a surface on an impinging sound wave, and it is defined as the ratio of sound pressure to particle velocity normal to the surface. If the propagation medium is locally reacting, then the surface normal impedance is independent of the angle of incidence. However, if the medium is non-locally reacting, then the surface normal impedance is dependent on the angle of incidence.

The classical approximation[12,13] for the sound field due to a point source above a surface or ground cannot be solved directly, but according to the well known outdoor sound theory of Weyl Van der Pol, numerical fitting methods can be used. Attenborough[14,15] developed a five-parameter model to predict the acoustical characteristics of rigid fibrous absorbent soils. The five parameters were porosity, flow resistivity, tortusity, steady flow shape factor and dynamic shape factor. In 1992, Attenborough simplified his previous model and developed a two-parameter approximation for the normal surface impedance of a non hard-backed layer medium. The two parameters were porosity and flow resistivity. The values of the parameters can be ascertained by direct measurements, as when a wide range of flow resistivity values

are measured under plane wave normal incidence conditions by the impedance tube method over the frequency range. Moreover, the numerical fitting of different parameter values can be used to measure the sound attenuation data. Indeed, many researchers use the Weyl van der Pol formulation[16] of the sound field above locally reacting boundary or non-locally reacting boundary conditions as a theoretical prediction model.

The boundary element method (BEM) can also be used to predict sound propagation, in particular from a line source, over a flat plane of inhomogeneous impedance. The application of the boundary element method to sound wave problems and in particular to the problem of acoustic scattering, is well known. The method involves calculating the wave field at points on the discretised boundary. Subsequently, the wave field outside of the boundary can be calculated by integration over the boundary according to Green's theorem. Actually, BEM is well developed for sound propagation over an inhomogeneous impedance flat surface. Moreover, some approximation methods have been presented for sound propagation over an impedance discontinuity flat surface. These methods are related to sound propagation from a point source in a homogeneous still atmosphere above flat locally reacting ground.

1.1.7 Experimental technique

1.1.7.1 Maximum length sequence system

The attenuation of a sound field can be measured by a system called the maximum length sequence (MLS). The surface normal specific acoustic impedance fully characterizes the acoustic behaviour of a surface. This impedance can be used to calculate the absorption coefficient for normal, oblique, or random incidence of sound. Any impedance measurement technique should be quick and reliable, cover a wide frequency range and be easily portable for use in-situ. Conventional methods such as standing wave tubes test only small samples, rely on the plane wave assumption, and

are sensitive to the mounting of the sample. The method applies classical sound propagation theory in combination with numerical fitting. Actually, sound propagation theory is valid for many applications. The surface impedance is deduced from measurements of the interference pattern between the direct and the reflected sound of a point source above the surface under investigation. The acoustical properties of the surface near grazing incidence of sound waves are the most sensitive.

Moreover, the numerical fitting method for measuring the normal specific acoustic impedance of a surface has been applied in laboratory and in-situ. Conventional absorbing materials and a resonant type absorbent lining have been investigated. The result for plane and homogenous samples compared well with impedance tube measurements. In addition, the effective impedance was obtained and can be used to calculate the absorption coefficient for the random incidence of sound waves. The result of the absorption was smaller than that from the reverberation room. It has been shown that the method also works for resonant type absorber linings.

In general, many researchers use the Weyl van der Pol theory to predict sound propagation from a point source over locally reacting ground and extended reaction ground[17,18,19]. In this thesis, I shall use the well-known outdoor sound propagation theory, which is known as the Weyl van der Pol formula[17], to predict the acoustic impedance of MPP absorbers with different angles of incidence. After predicting the sound attenuation of the absorber, outdoor sound experimental measurements will be carried out to compare with the theoretical prediction.

1.1.7.2 Impedance tube measurement

In the past, various methods were used to determine the absorption coefficient and surface impedance of samples in impedance tubes. The oldest and most time-consuming method is sampling of the standing waves in front of a specimen (the SWR

method)[22]. A quicker way of measuring was made possible by analysing the complex transfer function (TF) between two separated microphones[23]. Later, this method was simplified and only one microphone was used. At the same time, the precision of the analysis increased. In more advanced terms, the computation programme for the sound absorption of microperforated panel absorber is based on Maa's theory. It enables accurate definition of the geometrical parameters of microperforated panel construction according to practical requirements. Estimates are also given for impinging diffuse sound fields. Recently, Chung and Blaser[24] proposed a new method of impedance tube measurements of sound absorption using the transfer function between acoustic pressures at two locations. The new method is claimed to be better than the conventional standing wave ratio method. In the testing, the impedance tube test method was selected according to the ASTM C384-95 standing testing method for impedance and acoustical materials. This method only measures the absorption coefficient at normal incidence, and is also called standing wave method. A loudspeaker is used as a sound source to produce a standing acoustic wave in the tube of uniform cross section. The other end of the tube is terminated by the sample of material to be investigated.

1.2 Motivation of the Current Work

Outdoor sound propagation theory is commonly used in the determination of attenuation of a sound field over an impedance surface or ground. The classical theory for the sound field due to a point source above an impedance plane can be solved by the well-known Weyl van der Pol formula[13]. This has been used by many researchers for the formulation of sound field propagation over a locally or non-locally reacting boundary. In this study, a more general model is established for the absorption performance of different kinds of sound absorbers. The main purpose of the study is to realise the sound attenuation by interference effect and the sound absorption of the

sound absorbers based on the model. Literature surveys[14,15,16] show that although many researchers have investigated the sound attenuation of the sound field over an impedance plane, they have only used fibrous materials as the testing samples.

For sound attenuation above a microperforated panel (MPP) absorber, no reports have been found in detail. In addition, the sound absorption of the absorber based on outdoor sound theory has not been derived. Moreover, Maa's theory is not general enough because it just considers plane wave propagation without any interference effect between the direct and the reflected waves[4,6]. In real life, the sound generated from a point source is a spherical wave, and the sound absorption is influenced by the interference effect as well as the impedance of the absorber. These effects will be taken into account in the proposed theory, which shall be more general in MPP absorber absorption performance prediction. Outdoor sound measurement is conducted to determine the sound attenuation by interference effect above the sound absorbers. As shall be illustrated, the analytical model can be applied to various types of sound absorbers.

1.3 Merit of the Research Work

For research studies of sound absorbers, sound attenuation and the absorption coefficient are the major factors in noise control engineering. In recent years, many researchers have investigated only one aspect in detail. In this study, a more general model is established for the evaluation of sound attenuation and the absorption coefficient by outdoor sound theoretical prediction. This will allow us to fully understand the acoustical characterisation of various types of sound absorbers.

Especially in relation to the micro-perforated panel (MPP) absorber, Dr. Dah-You Maa has only considered the normal incidence of sound waves propagated into the absorber[1]. In general, the sound wave propagates in oblique incidence or random

incidence. In addition, Maa has published research papers that provide the theoretical prediction of oblique acoustic impedance of the MPP absorber[4,20]. However there is no experimental result to validate this prediction. Thus, the oblique acoustic impedance of the MPP absorber is not rigorous.

Although Maa's theory is very famous in sound absorption treatment engineering, the oblique acoustic impedance of the theory has not been validated yet. As outdoor sound propagation is very popular to use for characterising the acoustic impedance of various sound absorbers with different incident angles of sound waves, the outdoor sound theory is applied for the numerical validation. In our study, we have to establish the acoustical properties of the MPP absorber for validation by outdoor sound theory. Actually, there are many different methods for deducing the acoustical characterisation of sound absorption materials from propagation measurements, all of which are effectively applicable[25,26,27].

References

(1) Biot, M.A. "Theory of elastic waves in a fluid saturated porous solid. II. Higher frequency range". *Journal of the Acoustical Society of America*, Vol. 28, pp.179-91 (1956)

(2) Attenborough, K. "Acoustical characteristics of rigid fibrous absorbents and granular materials". *Journal of the Acoustical Society of America*, Vol. 73, pp.785-99 (1983)

(3) Deleny, M.E. and Bazley, E.N. "Acoustical properties of fibrous absorbent materials". *Applied Acoustics*, p.3 (1970)

(4) Maa, D.Y. "Potential of microperforated panel absorber". *Journal of the Acoustical Society of America*, Vol. 104 No.5, (1998)

(5) Maa, D.Y. "Design of microperforated panel constructions". *Acta Acustica*, Vol. 13 No.3, (1988)

(6) Maa, D.Y. "Microperforated panel at high sound intensity". *Inter-noise 94*, Vol. 3, pp.1511-1514 (1994)

(7) Maa, D.Y. "Wide-Band sound absorber based on microperforated panels". *Chinese Journal of acoustics*, Vol. 4, p.3 (1985)

(8) Maa, D.Y. "Microperforated panel wideband absorbers". *Noise control engineering journal*, Nov.-Dec. (1987)

(9) Zhang, Z.M. and Gu, X.T. "The theoretical and application study on a double layer microperforated sound absorption structure". *Journal of sound and vibration*, Vol. 215 No.3, pp.399-405 (1998)

(10) Fromhold, W. , Fuchs, H.V. and Sheng, S. "Acoustic performance of membrane absorbers". *Journal of sound and vibration*, Vol.170 No.5, pp.621-636 (1994)

(11) Wu, M.Q. "Micro-perforated panels for duct silencing". *Noise control engineering Journal*, Vol. 45 No.2, Mar-Apr. (1997)

(12) Chien, C.F. and Soroka, W.W. "Sound propagation along an impedance plane". *Journal of sound and vibration*, Vol. 43, pp.9-20 (1975)

(13) Chien, C.F. and Soroka, W.W. "A note on the calculation of sound propagation along an impedance surface". *Journal of sound and vibration*, Vol. 69, pp.340-343 (1980)

(14) Howorth, C. "*Sound propagation over rigid porous layers*". Open University, Walton Hall, Milton Keynes, UK (1991)

(15) Attenborough, K. "Acoustical Characteristics of rigid fibrous absorbents and granular materials". *Journal of the Acoustical Society of America*, Vol. 73 No.3, March (1983)

(16) Attenborough, K. "Ground parameter information for propagation modeling". *Journal of the Acoustical Society of America*, Vol. 92 No.1, July (1992)

(17) Li, K.M. , Fuller, T.W. , and Attenborough, K. "Sound propagation from a point source over extended-reaction ground". *Journal of the Acoustical Society of*

America, Vol. 104 No.2, August (1998)

(18) Chien, C.F. and Soroka, W.W. "Sound propagation along an impedance plane". *Journal of sound and vibration*, Vol. 43 No.1, pp.9-20, (1975)

(19) Li, K.M. , Taherzadeh, S. and Attenborough, K. "Sound propagation from a dipole source near an impedance plane". *Journal of the Acoustical Society of America*, Vol. 101 No.6, June (1997)

(20) Kang, J. and Fuchs, H.V. "Predicting the absorption of open weave textiles and micro-perforated membranes backed by an air space". *Journal of sound and vibration*, Vol. 220 No.5, pp.905-920 (1999)

(21) Sakagami, K. , Nakanishi, S. and Daido, M. "M.Morimoto,'Reflection of a spherical sound wave by an infinite elastic plate with an air-back cavity". *Acustica*, Vol. 83, pp.963-971 (1997)

(22) Chu, W.T. "Extension of the two-microphone transfer function method for impedance tube measurements". *Journal of the Acoustical Society of America*, Vol. 80 No.1, July (1986)

(23) Kruger, J. and Quickert, M. "Determination of acoustic absorber parameters in impedance tubes". *Applied Acoustics*, Vol. 50, No.1 pp.79-89 (1997)

(24) Cha, X. , Jian, K. , Zhang, T. , Zhou, X. and Fuchs, H. "Application approach for microperforated panel sound absorbers". *Acta Acustica*, Vol. 19 No.4, July (1994)

(25) Li, J.F. "Use of pseudo-random sequences and a single microphone to measure surface impedance at oblique incidence". *Journal of the Acoustical Society of America*, Vol. 102 No.4, October (1997)

(26) Nocke, C. , Mellert, V. , Fuller, T.W. , Attenborough, K. and Li, K.M. "Impedance deduction from broad-band, point-source measurements at grazing incidence". *Acustica*, Vol. 83, pp.1085-1090 (1997)

(27) Nocke, C. "In-situ acoustic impedance measurement using a free-field transfer function method". *Applied Acoustics*, Vol. 59, pp.253-264 (2000)

CHAPTER 2

Theoretical Model of Sound Absorption Materials

2.1 Introduction

As have been mentioned in Chapter 1, there are two main types of sound absorbers that will be studied in the present thesis: fiberglass absorbers and micro-perforated panel absorbers. Acoustical characterisation of sound absorbers is a significant theme in noise control engineering field. The specific surface impedance and absorption coefficient are two major acoustical properties of sound absorption materials. The principal objective of this chapter is to establish a general analytical model for the estimation of sound propagation over the sound absorbers. This, in turn, allows the determination of their absorption coefficient.

Pyett[1] developed an analytical model based on particular impedance model to evaluate the acoustic surface impedance of a porous layer at oblique incidence. Some impedance measurements at oblique incidence had been made and showed good agreements with theoretical prediction. Chien and Soroka[2] proposed an asymptotic approximation for calculating sound field due to a point source above an impedance plane. The asymptotic solution for the sound field was obtained by a double saddle point method of integration. Li *et al.*[3] extended their model for computing the sound field due to point source above an extended reaction ground. Their impedance ground model included a semi-infinite, a hard-backed layer and a double layer. Their theoretical prediction of sound fields due to a point source over these ground models showed good agreements with the experimental results. In recent years, Nocke *et al.*[4] introduced a numerical method that was based on the inversion of the Weyl-Van der Pol formula for

determining the acoustic impedance of ground surfaces. The surface impedance was obtained by fitting complex excess attenuation measurements. The new technique does not require the assumption of any particular impedance model.

The absorption coefficient is one of important acoustical properties of sound absorbers. Delany and Bazley[5] proposed a model for characterising the acoustical properties of sound absorption materials based on an empirical power-law relationship. The impedance tube measurement over frequency range of practical interest was conducted to determine the normal impedance and propagation coefficient of the absorption materials. Also the energy absorption coefficient of normal incidence of the absorption materials was derived from the normal impedance measurements. A semi-infinite of one parameter model was developed. Recently, Wang and Torng[6] have published a technical note about the absorption characteristics of some porous fibrous materials. The flow resistivity and the absorption coefficient of the fibrous materials are obtained in experimental measurements. The theoretical prediction is based on a proposed model by Allard *et al*[7]. The dynamic density and bulk modulus can be evaluated and consequently the characteristic impedance and the propagation constant can also be obtained.

In the present study, an analytical model based on outdoor sound propagation theory proposed by Li *et al.*[3] is used in the analysis. The characterisation of surface impedance as a function of flow resisivity is determined by numerical fitting of excess attenuation measurements. Thus the prediction of sound fields due to a point source over the fiberglass absorbers can be obtained. Also the numerical evaluation of average absorption coefficient of the absorbers is derived and the technique is a similar approach to Delany and Bazley[5] model. Ingard[8] indicated that the plane wave is usually simulated by the more or less spherical wave obtained far from the sound source. It is quite

impossible to obtain plane wave conditions with any accuracy for angle of incidence larger than approximately 80°. If the sound source is generated very close to the impedance surface, the complex reflection coefficient should be multiplied by boundary loss factor. This model may evaluate the average absorption coefficient of spherical wave conditions as well as predict the sound fields due to point source over the absorbers. The limitation of plane wave conditions over the absorbers may be eliminated based on the proposed theory.

2.2 Sound Propagation over an Impedance Plane

For outdoor sound propagation prediction, a useful model is to consider a two-media problem with the plane interface lying at $z = 0$ in a rectangular co-ordinate system with x and y as the horizontal axes and z as the vertical axis, see Figure 1. The acoustic pressure field p over impedance surface due to a point monopole source can be represented by the Helmholtz equation below,[9]

$$\nabla^2 p + k^2 p = -\delta(x)\delta(y)\delta(z - z_s) \tag{1}$$

where k is the wave number and the source is located at (0, 0, z_s). The solution of Eq. (1) is also required to satisfy the boundary condition at $z = 0$,

$$\frac{\partial p}{\partial z} + ik\beta p = 0 \quad , \tag{2}$$

where β is the specific normalized admittance of the impedance plane. To find the solution for the inhomogeneous Eq. (1), it is convenient to introduce a Fourier transform pair as follows.

$$\hat{p}(k_x, k_y, z) = \int_{-\infty}^{\infty} \int_{-\infty}^{\infty} p(x, y, z) e^{-ik_x x - ik_y y} dx dy \tag{3}$$

and

$$p(x,y,z) = \frac{1}{4\pi^2}\int_{-\infty}^{\infty}\int_{-\infty}^{\infty}\hat{p}(k_x,k_y,z)e^{ik_x x+ik_y y}dk_x dk_y \quad . \tag{4}$$

Substituting Eq. (3) into Eqs. (1) and (2), we can express the Helmoltz equation in terms of the transformed pressure, $\hat{p}$ as

$$\frac{d^2\hat{p}}{dz^2} + k_z^2\hat{p} = -\delta(z-z_s) \tag{5}$$

where $k_z = \sqrt{k^2 - k_x^2 - k_y^2}$.

Application of the Fourier transform in the boundary condition of the impedance surface at $z = 0$, Eq. (2) becomes

$$\frac{d\hat{p}}{dz} + ik\beta\,\hat{p} = 0 \quad . \tag{6}$$

It is straightforward to obtain a solution for the transformed pressure $\hat{p}$, come from Eqs. (5) and (6), as follows:

$$\hat{p} = \frac{i}{2k_z}\left\{e^{ik_z|z-z_s|} + \frac{k_z - k\beta}{k_z + k\beta}e^{ik_z(z+z_s)}\right\} \quad . \tag{7}$$

Substitution of Eq. (7) into Eq. (4) and evaluation the integral asymptotically lead to a closed form analytical solution for computing the sound pressure. The details of the evaluation method has been described elsewhere [see, for example, Chien and Soroka[2]]. The sound pressure field can be calculated by the so-called Weyl-Van der Pol formula as

$$p = \frac{e^{ikr_1}}{4\pi r_1} + \left\{R_p + (1-R_p)F(w)\frac{e^{ikr_2}}{4\pi r_2}\right\} \tag{8}$$

where w is the numerical distance determined according to

$$w = (\frac{1}{2}ikr_2)^{1/2}(\cos\theta + \beta), \tag{9}$$

$F(w)$ is known as the boundary loss factor which is given by

$$F(w) = 1 + i\sqrt{\pi} w e^{-w^2} \operatorname{erfc}(-iw), \tag{10}$$

and R_p is the plane wave reflection coefficient that can be calculated according to

$$R_p = \frac{\cos\theta - \beta}{\cos\theta + \beta} \quad . \tag{11}$$

Also r_1 is the distance of the direct sound wave and r_2 is the distance of the reflected sound wave, see Figure 1. From Eq. (8), the sound pressure p is a sum of the two terms. We can easily interpret the solution of Eq. (8) with the first term corresponding to the direct wave. The second term is the contribution due to the reflected wave.

2.3 The Sound Field above a Fibrous Absorbent System

For the propagation of sound above a fibrous material absorber, we often employ the Weyl-Van der Pol formula as given in Eq. (8) to compute the sound field. However, an effective admittance β_e is used to replace the normalise admittance β of the numerical distance w and the plane wave reflection coefficient R_p. The effective admittance is given by[5]

$$\beta_e = \frac{1}{Z_{fiberglass}}$$

$$= m_1 \sqrt{n_1^2 - sin^2\,\theta} \tag{12}$$

where

$Z_{fiberglass}$ is the normal acoustic impedance of fiberglass absorber, $m_1 (\equiv \rho/\rho_1)$ and $n_1 (\equiv k_1/k)$ are ratios of complex density and propagation constant. The varibales ρ_1 and k_1 are, respectively, the complex density and propagation constant for the absorbent material. The variable ρ is the density of air and $k (\equiv \omega/c)$ the wave number.

Use of the Delaney and Bazley impedance model, the real and imaginary parts of complex propagation constant are given by

$$k_1/k = \left\{1 + 10.8(\sigma/f)^{0.70} + i\,10.3(\sigma/f)^{0.59}\right\} \tag{13}$$

where σ is the effective flow resistivity of the fibrous materials in cgs units (1 cgs unit = 1 kPa s m^{-2}), and f is the frequency. Moreover the normalized impedance of the fibrous materials are obtained by

$$Z_1 = 1 + 9.08(\sigma/f)^{0.75} + i\,11.9(\sigma/f)^{0.73} \tag{14}$$

where $Z_1 = \dfrac{1}{m_1 n_1}$. (15)

Also, the plane wave reflection coefficient and the numerical distance are given, respectively, by

$$R_p = \frac{\cos\theta - \beta_e}{\cos\theta + \beta_e} \tag{16a}$$

and $$w = \left(\frac{1}{2} ikR_2\right)^{1/2}(\cos\theta + \beta_e) \quad . \tag{16b}$$

For plane incident waves, the absorption coefficient α_θ can be calculated by use of the plane wave reflection coefficient to yield:

$$\alpha_\theta = 1 - \left|R_p\right|^2 = \frac{4\cos\theta\,\mathrm{Re}\left(Z_{fiberglass}\right)}{\left[1 + \cos\theta\,\mathrm{Re}\left(Z_{fiberglass}\right)\right]^2 + \left[\cos\theta\,\mathrm{Im}\left(Z_{fiberglass}\right)\right]^2} \quad . \tag{17}$$

In a diffuse sound field, a mean sound absorption coefficient α_0 can be obtained by angle-averaged of α_θ as follows,

$$\alpha_0 = 2\int_0^{\pi/2} \alpha_\theta \sin\theta\cos\theta d\theta \quad . \tag{18}$$

Although there is no simple closed form analytic expression, it is straightforward to compute α_0 numerically for different frequency bands.

However, we wish to point out that the spherical wave reflection coefficient should be used in place of the plane wave reflection coefficient for the calculation of the angle-averaged absorption coefficient if a point source is considered instead of a plane wave. In this case, not only is the absorption coefficient a function of the incident angle θ but it also depends on the source height h and the distance from the image source to the receiver r_2. The absorption coefficient is modified to

$$\alpha(\theta, h_s, r_2) = 1 - \left| R_p + (1 - R_p) F(w) \right|^2 \quad , \tag{19}$$

where the numerical distance w and the boundary loss factor $F(w)$ are given by Eqs. (9) and (10) respectively. A close examination of the source/receiver configuration (see Figure 2), we can give an analogue expression of the angle-averaged absorption coefficient for a given source height as

$$\alpha_h = \lim_{r_2 \to \infty} \left[2 \int_0^{\pi/2} \alpha(\theta, h, r_2) \sin\theta \cos\theta \, d\theta \right] \quad , \tag{20}$$

where θ is the averaged angles between 0 and $\pi/2$. We can further generalize the expression to allow for the case of a random incidence with noise sources located in the region $0 \le h \le H$,

$$\alpha_0 = \frac{1}{H} \int_0^H \alpha_h dh \quad . \tag{21}$$

2.4 Experimental Validation

To confirm the validity of the impedance model for fiberglass absorbers, we compare numerical predictions with experimental results. The experimental data are obtained by using (i) indoor standard ground characterisation measurements by MLSSA system and (ii) a standard impedance tube. We also compare our theoretical results with

experimental data that were obtained by others who conducted experiments in a standard reverberant chamber.

2.4.1 Principle of MLSSA System

Maximum Length Sequence System Analyser (MLSSA) is a single channel analyzer that can do the work of conventional dual-channel analyzers. As a result, it is much simpler to use and the cost of equipment is greatly reduced. The Maximum length sequence (MLS) stimulus has a low crest factor for a high signal energy content. Thus, MLS measurements provide very high signal-to-noise ratios. The MLSSA uses a special type test signal called a maximum length sequence, which is different from conventional white noise. The maximum length sequence is non-random, deterministic, periodic and exactly repeatable yet still remain most of the desirable characteristics of white noise. Therefore, there is no need to simultaneously measure the stimulus input with the system output as required by dual-channel FFT techniques. The deterministic nature of the MLS means that it can be pre-computed and need not to be measured simultaneously with the system response. The periodic nature of an MLS means that a single time-domain circular cross-correlation calculation can recover the complete system impulse response without the need for data tapering windows. So windowing error can be reduced while the entire period of the sequence is used to make the measurement which MLSSA does automatically.

2.4.2 Sound propagation over the fibrous materials

In the present study, it is suffice to use a Delaney and Bazley model[5] to model the impedance of the fiberglass. The real and imaginary parts of the impedance (Z_R and Z_X) and attenuation constants (K_R and K_X) are determined according to,

$$Z_R = 1 + 9.08(\sigma/f)^{0.75} \tag{22a}$$

$$Z_X = 11.9(\sigma/f)^{0.73} \tag{22b}$$

$$K_R = k\left[1 + 10.8(\sigma/f)^{0.70}\right] \tag{22c}$$

$$K_X = 10.3k(\sigma/f)^{0.59} \tag{22d}$$

where σ is the effective flow resistivity of the fiberglass in cgs unit (1 cgs ≡ kPa s m^{-2}), k is the wave number and f is frequency of the incident sound waves. Preliminary experiments suggest that a semi-infinite model[5] should be used because the density and thickness of the fiberglass are sufficient to prevent reflections from the backing wall. The effective impedance of the fiberglass is given by[3]

$$Z_f = \frac{1}{m\sqrt{n^2 - \sin^2\theta}} \tag{23}$$

where

$$mn = \frac{1}{Z_R + iZ_x} \tag{24a}$$

and $$n = \frac{K_R + iK_x}{k} \tag{24b}$$

Use of Eqs. (22 a-d) and (24a) and (24b) in Eq. (23), we can determine the acoustic impedance of the semi-infinite fiberglass. Excess attenuation spectra are plotted where the excess attenuation (EA) is defined as the total field relative to the reference field from the source to receiver:

$$\mathrm{EA} = 20\log\left|p\Big/\left(\frac{e^{ikr}}{4\pi r}\right)\right| \tag{25}$$

where r is the horizontal distance between the source and receiver.

In our experiments, two types of fiberglass samples with different flow resistivities and densities were tested. The parameters of sample 1 (pink) fiberglass

absorbers are density: ρ_1 = 48kg/m^3; and thickness of fiberglass: D_f = 50mm. The parameters of the sample 2 (soft yellow) fiberglass absorber are density: ρ_1 = 16kg/m^3; and thickness of fiberglass: D_f = 50mm. The acoustical properties of these samples were firstly characterised inside the anechoic chamber of size 6 × 6 × 3 m (high). A Tannoy driver with a tube of 3 cm internal diameter and 1 m long was used as a point source in this experiment. The sound source was connected to a maximum length sequence system analyser (MLSSA) with an MLS card installed in a PC. The analyser was connected to a B&K 2713 amplifier. The MLSSA system was used both as the signal generator for the source and as the signal-processing analyser. A BSWA TECH MK224 1/2 inch condenser microphone and a BSWA TECH MA201 preamplifier were used together as the receiver. Both source and receiver were placed at a fixed position by means of a stand and clamps. The range between the source and receiver was fixed with only their heights adjusted for different sets of measurement. The experimental set-up of the fiberglass absorber is shown as Figure 3. The sound attenuation above the absorbers was measured for different configurations. During the experiments, the source and receiver were placed above and to each side of the sample 1 fiberglass absorbers with same height at 10 cm. The range of the source and receiver was 1 m. For the sample 2 fiberglass absorber, the height of the source and receiver were 5.5 cm and 23.5 cm respectively. The range of the source and receiver was 60 cm.

2.4.3 Numerical Results

Numerical evaluations of the sound fields due to a point source over fiberglass absorbers are obtained by using a MATLAB program. Compared with experimental data, the numerical results show good agreements. Typically results are shown in Figures 4 and 5.

The excess attenuation (EA) of the fiberglass absorbers can be established by subsitution of the acoustic oblique impedance of sound waves. Moreover, the acoustic impedance of the absorbers are determined by the numerical fitting method with the experimental results. Based on the Eq. (25), EA is determined as the total sound field is divided by reference sound field from source to receiver. In present study, the total field may be evaluated based on Weyl-Van der Pol formula and the reference field of Figure 4 and Figure 5 is the horizontal distance of 1 m and 0.6 m respectively between source and receiver.

As seen in Figure 4 and 5, the experimental results show good agreement with the theoretical prediction based on outdoor sound propagation theory. Consequently, best-fit parameters of the flow resistivity were 15000 Pa s m^{-2} and 9000 Pa s m^{-2} for the sample 1 and sample 2 fiberglass absorbers respectively.

2.4.4 Principle of impedance tube method

Impedance tube is sometimes used to measure the sound absorption coefficient, sound reflection coefficient and normalized impedance of a material. The sound absorption coefficient is defined as the fraction of non-reflected sound energy to the incident sound energy. The impedance tube method of measuring the sound absorption coefficient includes the decomposition of a broad-band stationary random signal into its incident and reflected components. The signal is generated by a sound source, and the incident and reflected components are determined from the relationship between the acoustic pressure measured by microphones at two locations on the wall of the tube. A plane wave travelling in one direction down a tube is reflected back by the test specimen to produce a standing wave that can be explored with a microphone. The

sound absorption coefficient is determined from the standing wave ratio at the face of the test specimen.

2.4.5 Normal incidence absorption coefficient

The impedance tube was used to measure the sound absorption coefficient of the fiberglass sample 1 and sample 2. The apparatuses of this experiment are the two-microphone impedance measurement tube B&K type 4206, power amplifier B&K type 2706, two specially designed 1/4 inch micrphones B&K type 4187 with preamplifiers, data acquisition front-end B&K type 2827, ethernet switch, a standard PC and pulse softtware. For the measurement in the low frequency range (40Hz-1600Hz), a large impedance tube with inner diameter of 100 mm was used; whilst the 29mm inner diameter samller tube was used for measurement in the high frequency range (160Hz-6400Hz). For the sample 1 fiberglass absorber, the parameters were flow resistivity: σ = 15 kPa s m^{-2}; thickness: D_f = 50 mm; and density: ρ_1 = 48 kg/m^3. For the sample 2 fiberglass absorbers, the parameters were flow resisivity: σ = 9 kPa s m^{-2}; thickness: D_f = 6 cm and 25 mm; and density: ρ_1 = 16 kg/m^3. The experimental set-up of these absorbers is shown in Figure 6.

2.4.6 Numerical Results

Absorption coefficient of the fiberglass may be evaluated numerically by Matlab program. In present study, the normal impedance of fiberglass absorber is determined by best-fit parameter of flow resistivity based on Weyl-Van der Pol formula. Thus, normal absorption coefficient may be evaluated straightforward after getting impedance parameter of fiberglass absorber based on Deleny and Bazley model. In Figure 7 and

Figure 8, it is seen that the experimental results of impedance tube method show good agreement with the theoretical prediction based on the proposed theory.

As shown in Figure 7, the normal absorption coefficient of sample 1 fiberglass absorber is as a function of frequencies. It is shown that the measured frequency range is up to 6400Hz for small impedance tube measurement. For variation of absorption coefficient against different frequencies, Figure 7 shows that the absorption coefficient of sample 1 is about 0.95 at 1000Hz and maintain the absorption performance up to 6400Hz. The absorption coefficient may be attained to 1 at certain frequencies (1500Hz and 4500Hz). Thus the useful frequency range for practical use is 1000Hz to 6400Hz. It is quite significant for sound absorption at high frequency range.

As seen in Figure 8, the normal absorption coefficient of sample 2 fiberglass absorber is as a function of frequencies. In Figure 8, it is shown that the measured frequency range is 100 to 6400Hz. For variation of absorption coefficient against different frequencies, Figure 8 observes that the absorption coefficient of sample 2 is about 0.5 at 1500Hz and increased gradually to 0.95 at 4000Hz. Thus the useful frequency range for practical use is 1500Hz to 4000Hz. However the absorption coefficient of frequency range from 100Hz to 1500Hz is below 0.5. It is not quite significant for sound absorption at such frequency range.

In general, many researhers considered normal absorption coefficient and excess attenuation individually. In present study, this is a more general theoretical method to predict the absorption coefficient of fiberlgass absorber as well as excess attenuation. It is no doubt that this model makes us more understanding the acoustic properties of fiberglass absorber based on the proposed theory.

2.4.7 Principle of Reverberation Room Testing

In real life situation sound waves propagate through the atmosphere and impinges obliquely onto the material surface. In order to simulate this situation and obtain more realistic data, the samples can be laid in the reverberation chamber to measure the absorption coefficient. The sound absorption coefficient is the percentage of incident sound energy that, rather than being reflected, is converted to other forms of energy such as heat. Using a reverberation room, the sound absorption is computed as the difference of the Sabine absorption with and without the samples under test present in the reverberation room. Also, the size of room is typically greater than 200 m^3. Generally, the one-third octave bands centered between 100Hz and 5000Hz. The frequency range of interest may be extended downward to the 63 Hz octave band in large chambers of concrete construction. Measurements require careful control of temperature and humidity, with which accurate measurements can be made out to 10 kHz. The sound absorption of the samples is the difference of the Sabine absorption measured in each band with the samples present and with the room empty. The sound absorption coefficient of the sample is computed by dividing the sample sound absorption by the sample area. The reverberation room testing method is very simple indeed.

2.4.8 Absorption coefficient for random incidence

Reverberation room measurements have been carried out in a laboratory at switzerland. The measurement is based on the assumption that the sound field in the reverberation room is diffuse. In this experiement, the sound absorption measurement included the principles and testing proceduces is depended on international acoustic standard of ISO 354 -1985. There is one types of fiberglass samples with different flow

resistivities were tested. The parameters of the sample 1 fiberglass absorbers are density: ρ_1 = 48kg/m^3; and thickness of fiberglass: D_f = 50mm.The size of reverberation room is 211 m^3 and the surface area is 12 m^2. Also, the temperature and relative humidity of the room is 20° and 60% respectively.

2.4.9 Numerical Results

Numerical integration for the average absorption coefficient of the fiberglass absorbers is evaluated by using the Matlab program and the experimental results are obtained by a standard reverberation room testing. The absorption coefficient of the absorbers is obtained by numerical summation of sound energy for random incidence of sound waves. This is defined as the ratio of the total sound energy absorbed to the total sound energy incidence. In Figure 9, it is shown that the sound absorption performance of sample 1 fiberglass absorbers for random incidence of sound waves is against frequency. Best-fit parameter of the flow resistivity was 15000 Pa s m^{-2} for the sample 1 fiberglass.

As seen in Figure 9, the average absorption coefficient of sample 1 is as a function of different frequencies. The measured frequency range is up to 5000Hz. It is shown that the trend of the numerical prediction for average absorption coefficient is very similar to the experimental results. Compared with the numerical prediction, the experimental deviation is large due to the limitation of edge effect by reverberation room testing. Thus the absorption coefficient obtained experimentally is typically greater than 1 at wide frequency range because of edge effect. Figure 9 shows that absorption coefficient at 700Hz starts to exceed 1 up to 5000Hz. The deviation of absorption coefficient between experimental results and numerical prediction is large and the difference of absorption coefficient is about 0.2. However, when absorption

coefficient is increased to 1000Hz, the absorption performance of sample 1 is steady. Thus, the deviation of absorption coefficient is reduced and the difference of absorption coefficient is about 0.2. Both experimental results and numerical prediction become constant and the deviation of absorption coefficient are still about 0.2 at frequency range 1000Hz to 5000Hz.

For the proposed theory, the location of source and receiver has been determined. In order to obtain the impedance of the fiberglass absorber, the best-fit parameter of flow resistivity is calculated by numerical fitting method based on Weyl-Van der Pol theory. Thus the average absorption coefficient in spherical wave condition can be obtained easily. Furthermore, the average absorption coefficient of the fiberglass absorber for a random incidence with sound sources located in certain range is presented.

As shown in Figure 10, the average absorption coefficient would be increased at mid and high frequencies when receiver is closer to the sound source. Since the sound diffusion for random incidence is not enough if the receiver is much closer, the absorption performance of sample 1 fiberglass is like normal incidence condition. In Figure 10, the distance of direct sound waves are 100m, 50m, 5m and the range of source height is 1m to 3m. In fact, the limitation of receiver position may be determined based on the proposed formula in present study. Under outdoor circumstance, the variation of averaged absorption coefficient of different sound absorbers can be obtained. Therefore, our proposed model of sound absorption is mainly depended on the height of source and the range between the source and receiver.

2.5 Discussion

On the basis of previous measurements, the acoustical properties of sound absorption materials are firstly characterised inside the anechoic chamber. Secondly, the

sound absorption coefficient is evaluated numerically and compared with experimental results obtained by impedance tube method and reverberation room measurement. Thus, the proposed model is developed based on outdoor sound propagation theory. In fact, the acoustical characterisation of sound absorbers may be carried out enough inside the anechoic chamber if this present model is fully developed to predict the average or normal absorption coefficient of the absorbers. Normally, there are many limitations of reverberation room testing. For measurement for average absorption coefficient, a standard reverberation room is required and the size is typically not less than $200m^2$. The reverberation room size is very large and limited so there are not many laboratories which have this absorption testing room. Also it requires a large size of sample about $12m^2$ for testing each time. In fact, the acoustical performance of sound absorption materials is usually evaluated using the random incidence sound absorption coefficient, which can be measured in a reverberation room. However, this absorption coefficient is often affected by the combined influence of the diffusivity of the reverberation room and the area effect[10] or the edge effect[11] of the sample. The absorption coefficient often show values over 1.0, especially for highly absorbing materials or panels. Moreover, impedance tube measurement has just considered the plane wave propagation and is not commonly used for practical use. The normal absorption coefficient and impedance of the sound absorption materials can be deduced only.

Based on the present proposed analytical model, the acoustical impedance of the absorber has been firstly characterised under a quiet condition such as anechoic chamber. The sample size is needed about 2 (width) × 2 (length) m. The average and normal absorption coefficient may be obtained by numerical prediction. If the model is achieved experimentally and numerically, it is not required to carry out a lot of experimental measurements inside a reverberation room and using impedance tube.

Moreover, this is a more general analytical model because it includes sound attenuation by interference effect above the sound absorber and the energy sound absorption coefficient of the absorber.

In conventional theoretical method, the position of source and receiver is typical assumed as infinity and the model considers averaged angle absorption coefficient in plane wave condition only. However, in real case, sound waves propagate in spherical waves condition above the absorber if the position of receiver is located close to the source. Thus, this proposed theory is more general and makes us understand the average absorption performance in spherical wave condition and the constraint of the distance between source and receiver.

In present study, although we have not considered the cases in enclosed space and complicated surface. However, our proposed theory can also determine the sound attenuation and absorption coefficient of the surface in free field condition if we can clarify the impedance model and the position of the source and receiver above the complicated surface. Therefore, the theoretical result can be obtained based on our proposed theory.

2.6 Conclusions

In this chapter, an general analytical model is presented based on outdoor sound propagation theory. This proposed model includes sound attenuation and absorption coefficient of the fiberglass absorbers. The numerical evaluation for the sound absorption coefficient due to a point source over a fiberglass absorber is derived. If the sound source is very close to the fiberglass absorber, the sound waves propagation may be simulated as spherical wave condition. The sound fields due to a point source and absorption performance of the fiberglass absorbers may be determined based on the

proposed theory. Also, this model is a convenient tool to design sound absorber for outdoor and indoor environmental use.

References

(1) Pyett, J.S. "The Acoustic Impedance of A Porous Layer At Oblique Incidence". *Acoustica*, Vol. 3, pp.375-382 (1953)

(2) Chien, C.F. and Soroka, W.W. "Sound propagation along an impedance plane". *Journal of sound and vibration*, Vol. 43, pp.9-20 (1975)

(3) Li, K.M. , Fuller, T.W. and Attenborough, K. "Sound propagation from a point source over extended-reaction ground". *Journal of the Acoustical Society of America*, Vol. 104 No.2, August (1998)

(4) Nocke, C. , Mellert, V. , Fuller, T.W. , Attenborough, K. and Li, K.M. "Impedance deduction from broad-band, point-source measurements at grazing incidence". *Acustica*, Vol. 83, pp.1085-1090 (1997)

(5) Deleny, M.E. and Bazley, E.N. "Acoustical properties of fibrous absorbent materials". *Applied Acoustics*, p.3 (1970)

(6) Wang, C.N. and Torng, J.H. "Experimental study of the absorption characteristics of some porous fibrous materials". *Applied Acoustics*, Vol. 62, pp.447-459 (2001)

(7) Allard, J. F. , Champoux, Y. "New empirical equations for sound propagation in rigid frame fibrous materials". *Journal of the Acoustical Society of America*, Vol. 91, pp.3346-53 (1992)

(8) Ingard, U. "On the reflection of a spherical sound wave from an infinite plane". *Journal of the Acoustical Society of America*, Vol. 23(3), May (1951)

(9) Li, K.M. , Taherzadeh, S. and Attenborough, K. "Sound propagation from a dipole source near an impedance plane". *Journal of the Acoustical Society of America*, Vol. 101 No.6, June (1997)

(10) Maekawa, Z. and Lord, P. "Environmental and architectural acoustics". UK: E&FN SPON, pp.125-126 (1995)

(11) Kosten, C.W. "International comparison measurements in the reverberation room". *Acustica*, Vol. 10, pp.400-11 (1960)

Figures

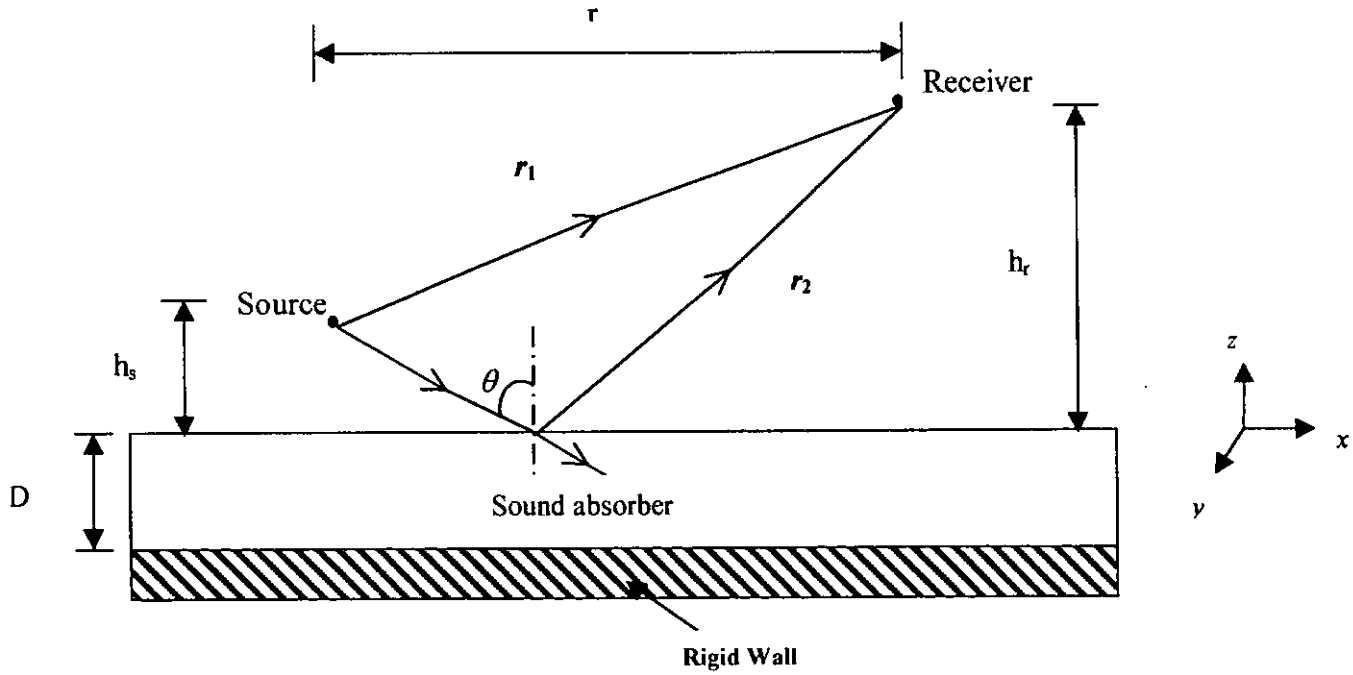

Figure 1 Schematic diagram of outdoor sound propagation model with x and y as the horizontal axes and z as the vertical axis.

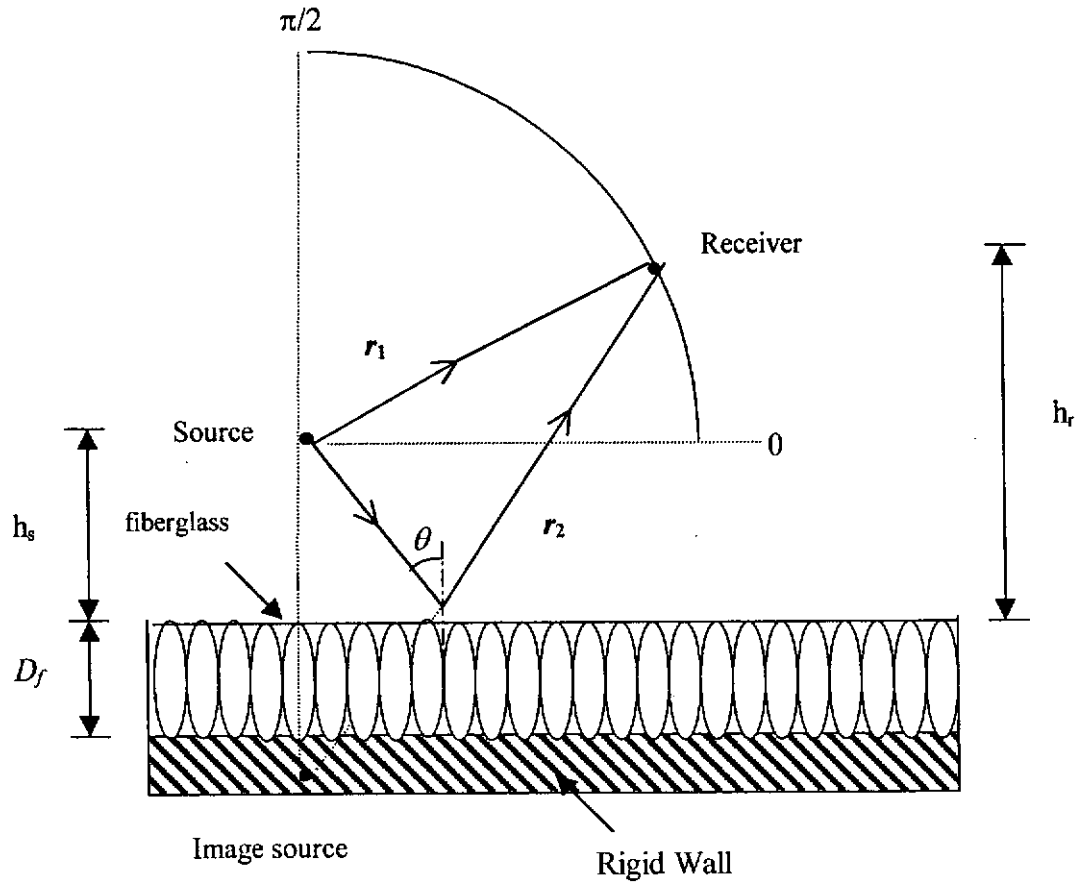

Figure 2 Schematic diagram of sound absorption over the fibrous absorber.

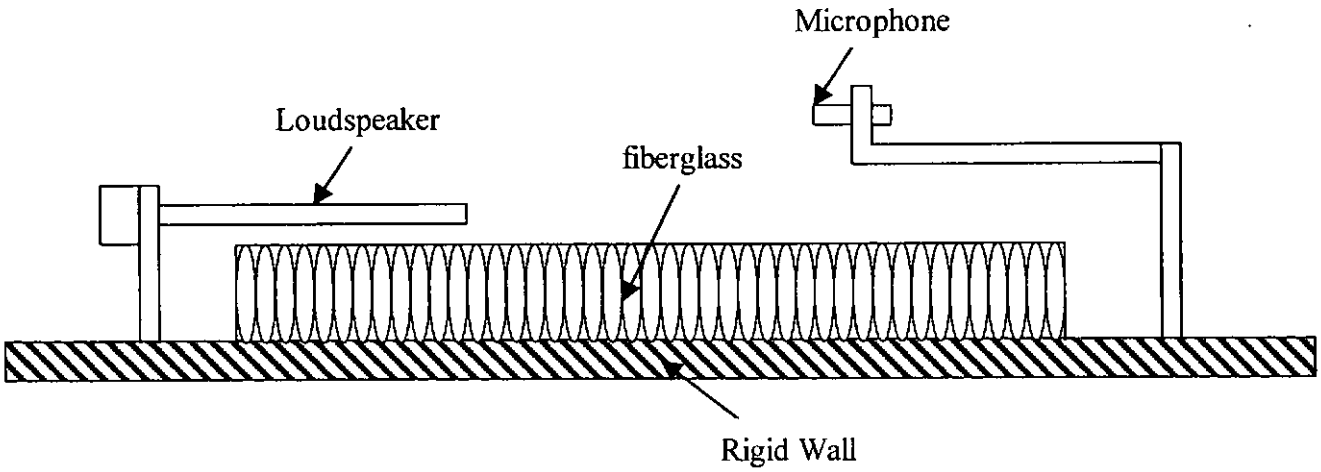

Figure 3 Schematic diagram of the experimental setup of fiberglass absorber.

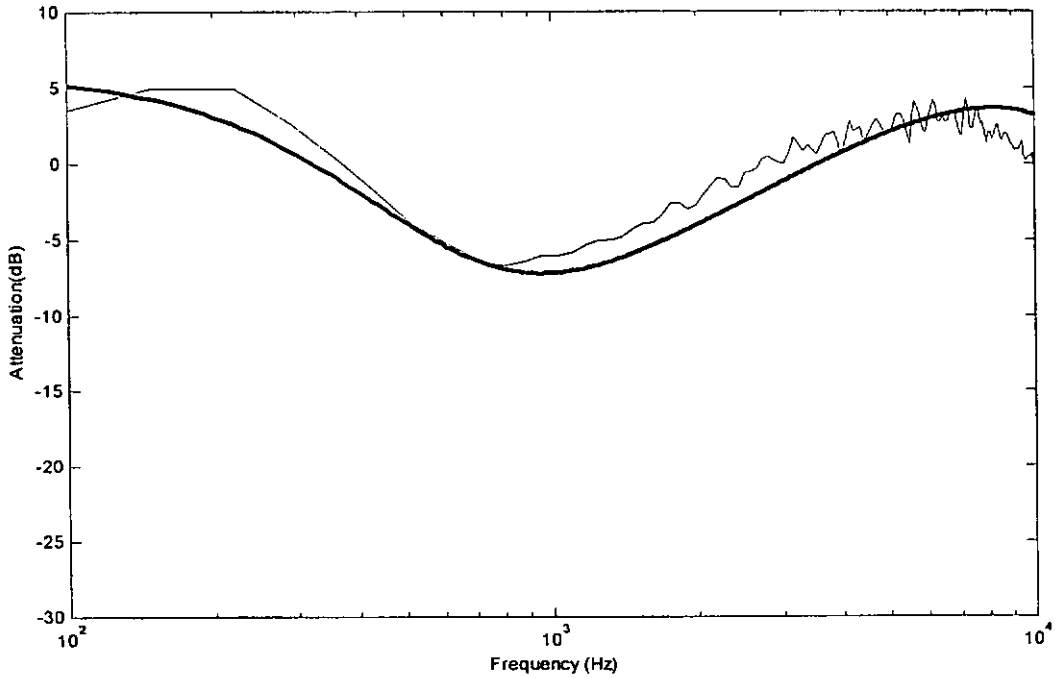

Figure 4 For sample 1, Attenuation data obtained with source height = 10cm, receiver height = 10cm and range = 1m.
Experimental result (solid line) and theoretical result (thick solid line)

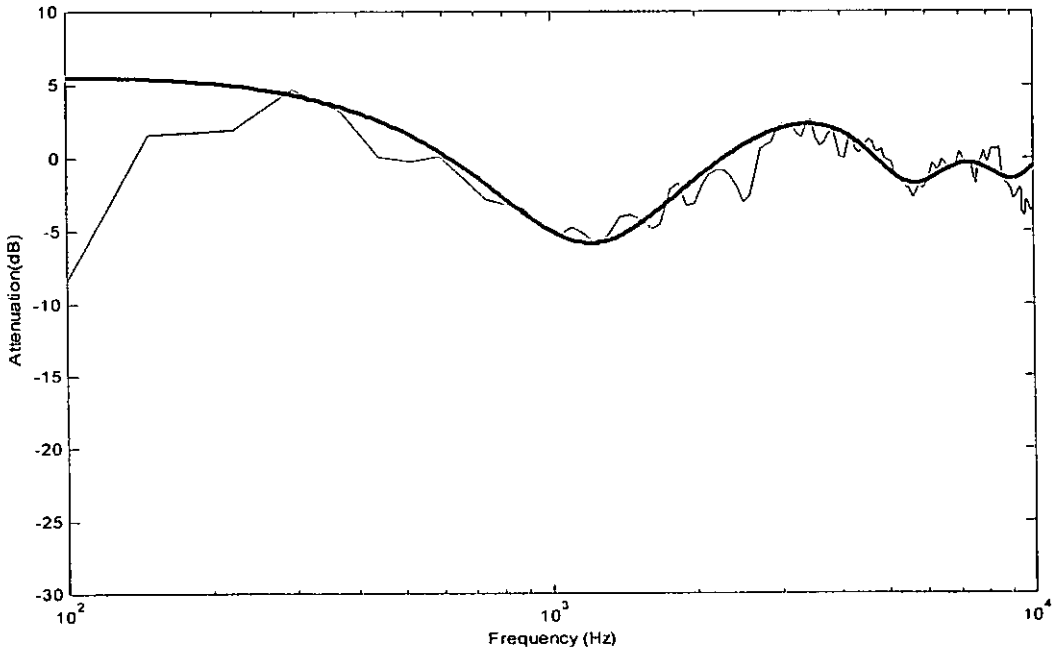

Figure 5 For sample 2, Attenuation data obtained with source height = 5.5cm, receiver height = 23.5cm and range = 0.6m.
Experimental result (solid line) and theoretical result (thick solid line)

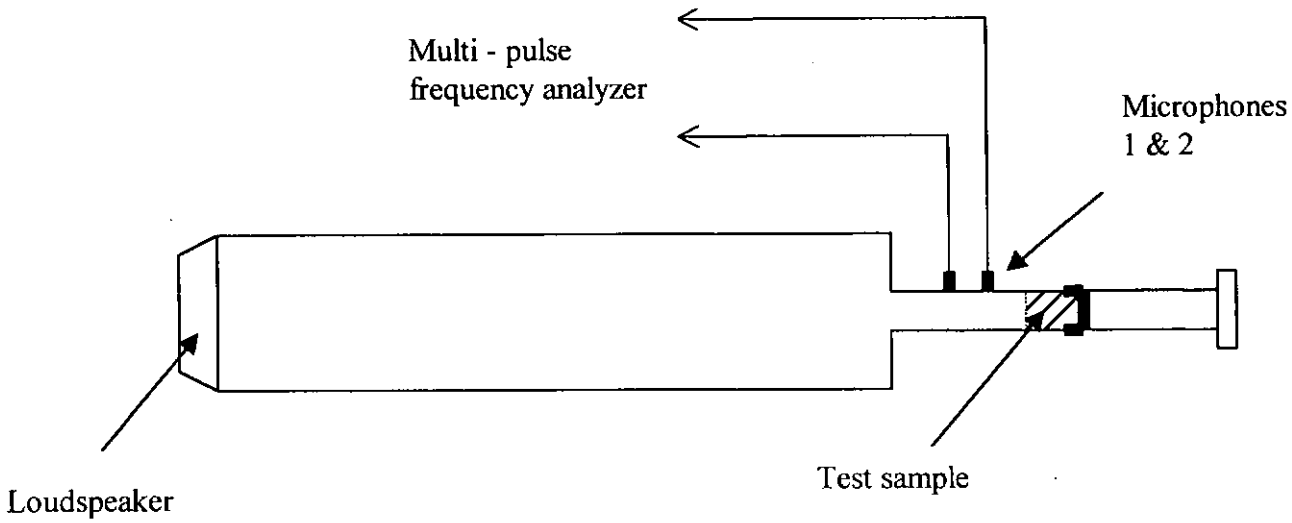

Figure 6 Experimental setup for small impedance tube measuerment.

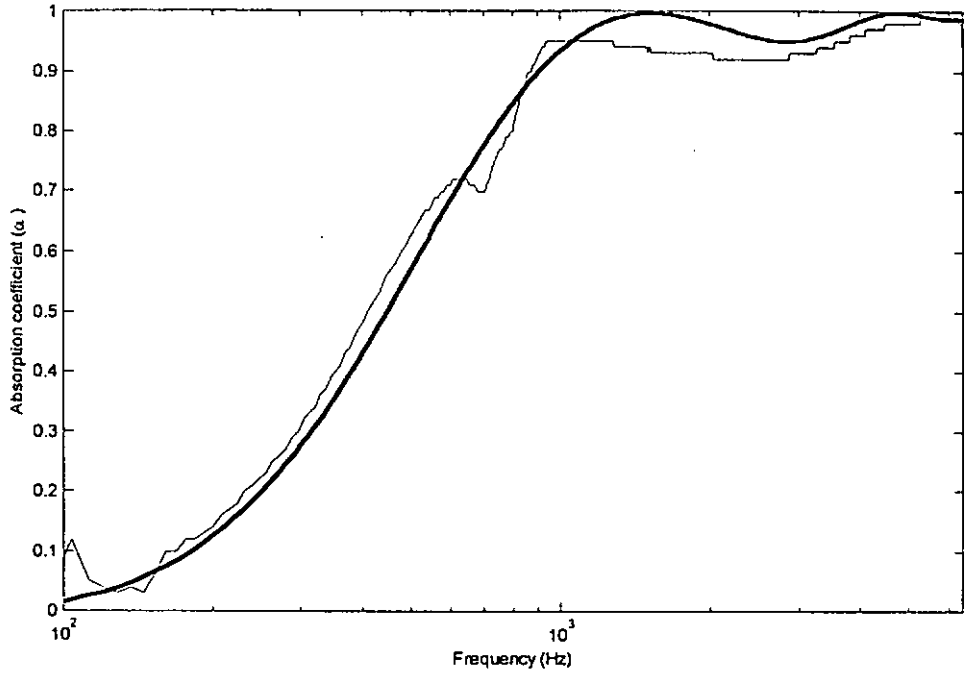

For small impedance tube measurement:
Figure 7 Absorption coefficient of sample 1 fiberglass absorber against different frequencies. Experimental result (solid line) and theoretical result (thick solid line) for thickness is 50mm.

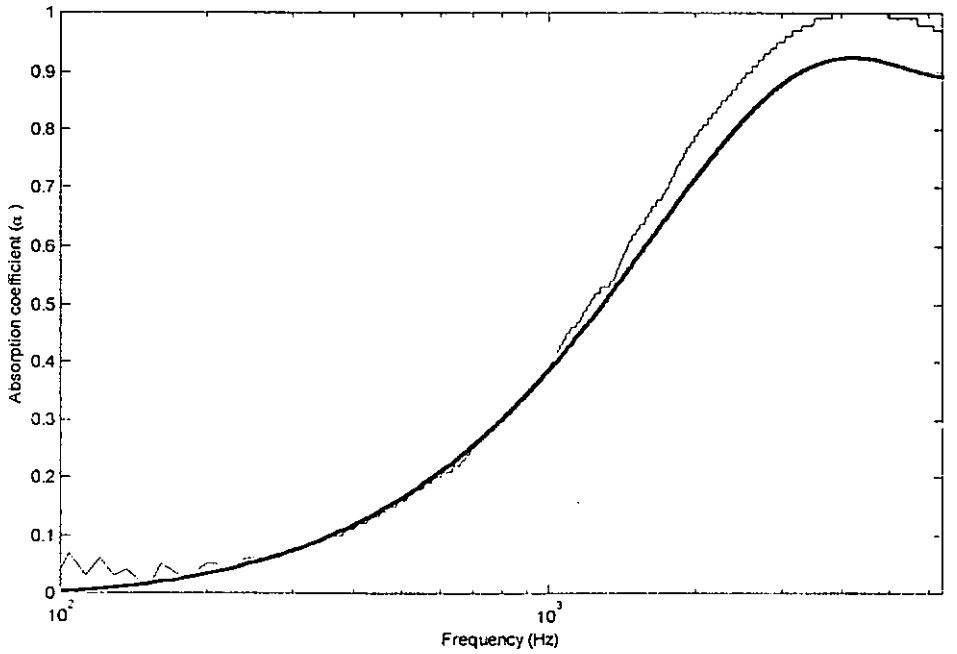

For small impedance tube measurement:
Figure 8 Absorption coefficient of sample 2 fiberglass absorber against different frequencies. Experimental result (solid line) and theoretical result (thick solid line) for thickness is 25mm.

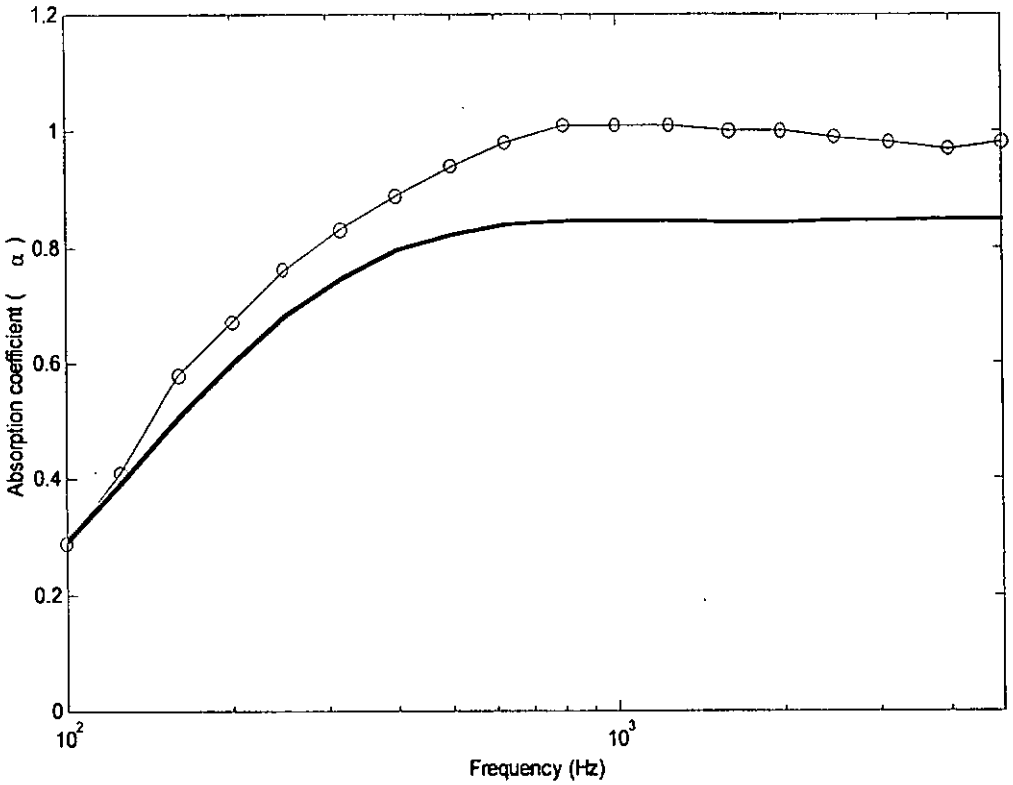

Figure 9 Average Absorption coefficient of sample 1 fiberglass absorber against different frequencies.
Experimental result of average absorption coefficient for random incidence of sound waves (solid line)
Numerical result of average absorption coefficient for random incidence of sound waves (circle)

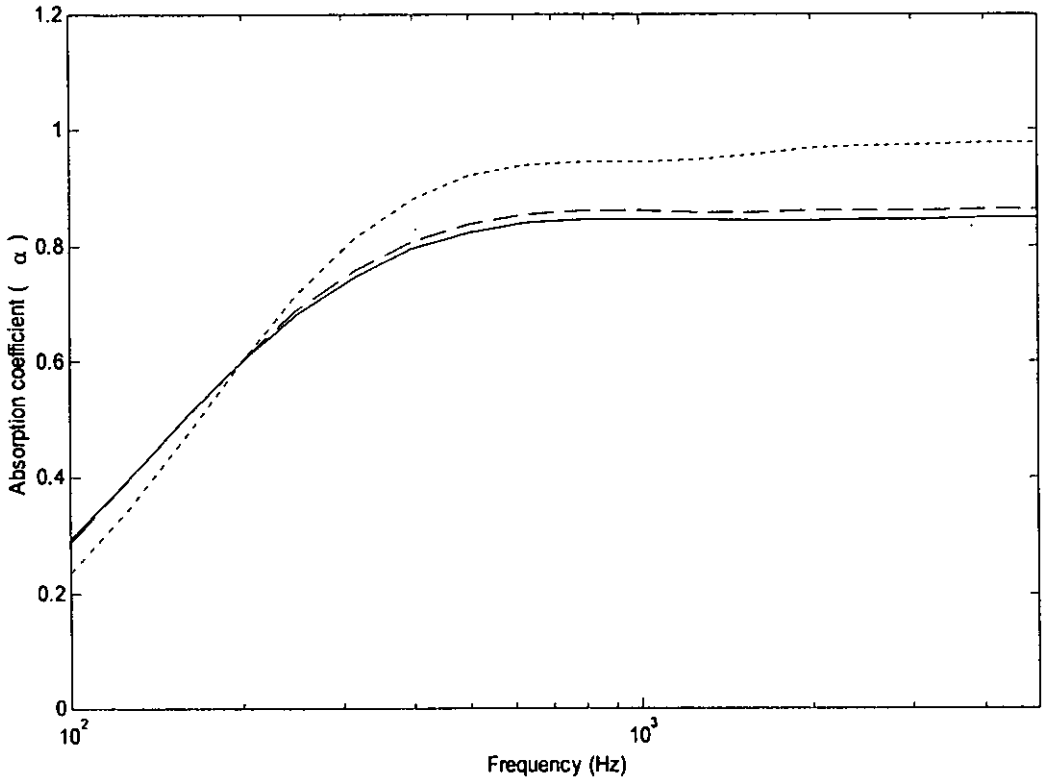

Figure 10 Absorption coefficient of fiberglass absorber for random incidence of sound waves.
Theoretical result (solid line) where $r_1 = 100$m and $1<h_s<3$.
Theoretical result (dashed line) where $r_1 = 50$m and $1<h_s<3$.
Theoretical result (dot line) where $r_1 = 5$m and $1<h_s<3$.

CHAPTER 3

Theoretical Model of Micro-Perforated Panel Absorber

3.1 Introduction

In Chapter 2, an analytical model based on outdoor sound propagation theory is established. This model is more general because it includes sound attenuation over the sound absorption materials and the absorption performance of the absorption materials. The first objective of this chapter is to predict the sound fields over micro-perforated panel (MPP) absorber and investigate the absorption performance of the MPP absorber based on the proposed theory. The second objective is to consolidate the acoustic impedance of MPP absorber for oblique incidence of sound waves.

Acoustical characterisation of sound fields due to a point source over the MPP absorber is presented. In literature survey, no report has been found for this topic. In previous studies, many researchers investigated the acoustical absorption performance and designed a MPP absorber. Maa[1] suggested that if the diameter of perforated panel was reduced to between 0.1 and 1mm. The sound absorber had high enough acoustic resistance and low mass reactance for sound absorption. The absorber was known as micro-perforated panel. After a few years, Maa[2] indicated that the frequency band of sound absorption was dependent on the diameter of perforations. Also, he suggested that a double layer MPP absorber extended the absorption to lower frequencies. The absorption also extended to higher frequencies when the MPP absorber was used in a random field. Thus, Maa[3] proposed the design procedures and its construction factor. In recent years, Maa[4] has presented the formulas and curves for MPP absorber design. Also, Zhang and Gu[5] have proposed a model to evaluate the resonant and anti-resonant frequency of single and double layer MPP absorption structure. In recent years, Kang

and Fuchs[6] have developed a theoretical method for predicting the absorption of open weave textile and micro-perforated membranes backed by an air cavity. The predictions for both normal and random incidence have shown very good agreement with experimental measurements. In the present study, the impedance Maa's model of MPP absorber will be validated experimentally. The study makes us further understand the absorption performance of the MPP absorber for random incident of sound waves.

Recently, Liu *et al*[7] investigated the sound absorption characteristic in diffuse sound fields experimentally. Some measurements of the absorption characteristics of the MPP absorber have been carried out in the impedance tube and reverberation room. Also, measurements of mixed construction (for example, MPP absorber is filled with fiberglass in the cavity) absorbers were made. The purpose is to compare and find the relation of normal and random incidence. However, there is no theory for predicting the absorption performance of mixed construction MPP absorber. In the present study, a theoretical method is presented for predicting the acoustic performance of a mixed construction MPP absorber. To validate the proposed theory, experimental measurements of sound attenuation and absorption coefficient have been carried out in an anechoic chamber and using impedance tube respectively. This chapter establishes a general analytical model based on Maa's theory. The prediction of sound fields due to a point source over the MPP absorbers can be obtained. Also, the numerical evaluation of normal and average absorption coefficient of the MPP absorbers is derived. The theoretical prediction from the present model shows a good agreement with both our and Liu *et al*[7] experimental results.

3.2 Theoretical model of the Impedance of Micro-Perforated Panel Absorber

The fundamental feature of a micro-perforated panel (MPP) absorber is a thin plate back by an air space. The thin plate, which has many small holes with diameters of 1 mm or less, can be made from a range of different materials from polyurethane to sheet metal and from plastic to plywood. The distances of adjacent apertures are small compared to the wavelength of incoming sound waves but are considerably larger compared to the aperture diameters. Essentially, the sub-millimeter size apertures offer considerable acoustic resistance and sufficient low acoustic mass reactance necessary for the absorption of wide-band sound. The theory for the absorption characteristic of micro-perforated panel absorbers is well studied[1-3] and the details will not repeated here. A brief review of the impedance model is outlined below.

According the Maa, a micro-perforated panel absorber is modeled by a lattice of narrow tubes embedded in a thin plate. Its normalized specific acoustic impedance for normal incidence is calculated by,

$$Z = R + iX \tag{1}$$

where R and X are the resistive and reactive components respectively. They are given by

$$R = \frac{32\mu t}{\phi \rho c d^2}\left\{\left(1+\frac{\varsigma^2}{32}\right)^{\frac{1}{2}} + \frac{\sqrt{2}}{8}\varsigma\frac{d}{t}\right\} \tag{2a}$$

$$X = \frac{2\pi f t}{\phi c}\left\{1+\left(9+\frac{\varsigma^2}{2}\right)^{-\frac{1}{2}} + 0.85\frac{d}{t}\right\} \tag{2b}$$

where ρ and μ are the air density and its coefficient of viscosity, c is the speed of sound in air, t is the thickness of the panel, d is the aperture diameter, ϕ is the ratio of

the perforated area to the total panel area, f is the frequency of impinging sound and ς is a shorthand notation for

$$\varsigma = d\sqrt{\frac{\rho\pi f}{2\mu}} \quad . \tag{3}$$

The parameter ς, may be termed as the perforate constant, as it is proportional to the aperture diameter and viscous boundary layer thickness inside the tube.

Together with the air cavity of depth D, the micro-perforated panel forms a resonant system. The normalized specific acoustic impedance, z_D of the air behind the thin plate, again at the normal incidence, is given by[1]

$$z_D = -i\cot(kD) \ , \tag{4}$$

where $k(=2\pi f/c)$ is the wave number of the impinging sound. The acoustic impedance of a micro-perforated panel back by an air space can be found easily by use of the electro-acoustic analogy. The resonant system comprises of a mass-resistance element in series with the cavity reactance of the air gap, as shown in Figure 1. Hence, the total acoustic impedance at the normal incidence, is simply given by

$$Z = R + iX + z_D = R + i[X - \cot(kD)] \tag{5}$$

In the case of oblique incidence, the apertures are locally reacting elements in which the acoustic impedance is independent of the angle of incidence. Hence, when the sound wave is incident at an angle θ to the normal, the normalized specific acoustic impedance becomes

$$Z = R\cos\theta + iX\cos\theta \ . \tag{6}$$

On the other hand, the acoustic impedance of the air gap depends on whether the air space is partitioned, (for example, with a honeycomb structure) or unpartitioned. For a partition air space, its acoustic impedance is locally reacting and is given by Eq. (4). In our case, the air space is unpartitioned that leads to acoustic impedance of the air space

being dependent on the angle of incidence. With an oblique angle of incidence θ to the normal, the normalized specific acoustic impedance of the air gap is[1]

$$z_D = -\frac{i}{\cos\theta}\cot(kD\cos\theta) \tag{7}$$

As before, the total acoustic impedance of the resonant system is the sum of individual components leading to

$$Z_\theta = R\cos\theta + iX\cos\theta + z_D\cos\theta = R\cos\theta + i\left[X\cos\theta - \cot(kD\cos\theta)\right] \ . \tag{8}$$

Multiple micro-perforated panels together with their associated air cavities form a multiple resonator that can be designed to broaden the sound absorption particularly at lower frequency bands.[1-2] By use of an analogue electrical circuit[6], it is straightforward to derive the overall impedance of a multiple micro-perforated panel absorber. In this paper, it is suffice just to consider a double resonator by using two micro-perforated panels with the corresponding impedances of Z_1 and Z_2. The suffixes 1 and 2 denote the corresponding properties of the respective resonate systems. In this case, the equivalent electrical circuit is shown in Figure 2. The R_1 and X_1 are arranged in series with z_{D_1} which is in parallel with R_2, X_2 and z_{D_2}. The normalized specific acoustic impedance is

$$Z = R_1 + i\left[X_1 - \cot(kD_1)\right] + \frac{\cot^2(kD_1)}{R_2 + i\left[X_2 - \cot(kD_1) - \cot(kD_2)\right]} \tag{9}$$

for normal incidence, and

$$Z_\theta = R_1\cos\theta + i\left[X_1\cos\theta - \cot(kD_1\cos\theta)\right] + \frac{\cot^2(kD_1\cos\theta)}{R_2\cos\theta + i\left\{X_2\cos\theta - \left[\cot(kD_1\cos\theta) - \cot(kD_2\cos\theta)\right]\right\}} \tag{10}$$

for an oblique angle incidence.

Finally, we have also considered the case for the combination of a micro-perforated panel and the traditional fiberglass-type sound absorption material. This configuration is achieved by laying a micro-perforated panel on the fiberglass which, in

turn, lay on a hard reflecting surface, see Figure 3. For this arrangement, the normalized specific acoustic impedance is simply

$$Z_\theta = R\cos\theta + R_f + i\left(X\cos\theta + X_f\right) \tag{11}$$

where R_f and X_f are the real and imaginary parts of the normalized specific acoustic impedance of the fiberglass, $Z_f = R_f + iX_f$. The impedance of the fiberglass can be determined by a fairly standard technique described elsewhere.[8]

3.3 Sound Absorption of Micro-Perforated Panel Absorber

According to the proposed theory in section 2.3 of Chapter 2, the normal and averaged-angle absorption coefficient of micro-perforated panel absorber in spherical wave condition can be determined by the above impedance model. Thus, the details will not repeat here. However, we wish to point out the oblique impedance of micro-perforated panel is validated experimentally. The plane and spherical wave reflection coefficient of the absorber is obtained easily. Therefore, the absorption coefficient of micro-perforated panel absorber can be evaluated based on the proposed theory.

3.3.1 Sound Propagation over a Micro-Perforated Panel

In order to validate the impedance model of micro-perforated panel absorbers, an indoor measurement by MLSSA system is conducted inside an anechoic chamber. A stainless steel sheet of thickness, t, 0.15 mm is used for the fabrication of a micro-perforated panel with lattices of small holes of diameter, d, 0.3 mm each and the pitch of aperture centers, b, of 3 mm. This leads to the aperture area ratio ϕ of about 0.8%. Adjusting the cavity depth between the panel and the backing wall, we can create different resonant systems of different characteristic impedance. For a double layer, the

same panel design (*i.e.* $t = d = 0.3$ mm and $b = 3$ mm) is used for both layers but the cavity depths are different for these two layers.

The experimental testing on the micro-perforated panel (MPP) absorber was carried out in an anechoic chamber. The sound attenuation of the absorber was measured by the maximum length sequence (MLS) system. The principle of maximum length sequence system analyzers (MLSSA) has been mentioned in Chapter 2. The micro-perforated panel was made of stainless steel. The parameters of the absorber were diameter: d = 0.3 mm; pitch: b = 3 mm; thickness: t = 0.15 mm; and the cavity of the panel absorber: D = 120 mm.

The sound fields due to a point source over the single and double layer MPP absorber were determined inside a anechoic chamber of size 6 × 6 × 4 m (high). A Tannoy driver with a tube of 3 cm internal diameter and 1 m long was used as a point source in this experiment. The sound source was connected to a maximum length sequence system analyzer (MLSSA) with an MLS card installed in a PC. The analyzer was connected to a B&K 2713 amplifier. The MLSSA system was used both as the signal generator for the source and as the signal-processing analyzer. A BSWA TECH MK224 1/2 inch condenser microphone and a BSWA TECH MA201 preamplifier were used together as the receiver. Both source and receiver were placed at a fixed position by means of a stand and clamps.

The sound attenuation was measured for different configuration. In these experiments, the source and receiver were placed above and to each side of the micro-perforated panel absorber, with certain height and various receiver positions. The range of the source and receiver were 40 cm, 50 cm and 60 cm. Moreover, the double layer MPP absorber was tested for further validation. The experimental set-up of the MPP absorber for the single layer is shown in Figure 4(a), and for a double layer in Figure

4(b). The sound attenuation measurement of a mixed construction (MPP with fiberglass) absorber was also carried out in the chamber. The parameters of the mixed construction absorber were diameter: d = 0.3 mm; pitch: b = 3 mm; and thickness: t = 0.15 mm. The experimental set-up of the mixed construction absorber is shown in Figure 4(c).

To eliminate the effect of background noise, outdoor sound measurements have been conducted under a free field environment such as anechoic chamber. When doing the measurements in an anechoic chamber, some problems of experimental setup has been encountered. In the experimental testing, the MPP is made of thin stainless steel metal and the minimum requirement size of MPP is 2m (width) x 2m (length). If the size of the metal MPP plate is less than 2m (width) x 2m (length), the experimental error may be occurred because of diffraction effect at the edge. In fact, it is difficult to make the large size of MPP plate flat and control the distance of air cavity between the MPP plate and rigid ground. To overcome the problem, the MPP plate has to be cut into four pieces and the size of each piece is 1m (width) x 1m (length). Also, each piece of MPP plate is clamped tightly and is combined into a large piece of MPP plate, see Figure 5-6. Thus, the distance of air cavity between the MPP plate and rigid ground may be controlled easily. As a result, a desired result is obtained in our measurements.

The numerical evaluation of sound attenuation over single layer metal MPP absorber, double layer MPP absorber and mixed construction MPP absorber is obtained by Matlab program. The proposed model shows good agreement with the experimental results.

The sound attenuation over stainless steel MPP absorber, double layer MPP absorber and mixed construction MPP absorber as a function of frequencies is shown as Figure 7-9. As shown in Figure 7-9, several dips appear with sound attenuation against frequencies. These dips can be classified into two types.

First, there are significant dips that appear at the lowest frequency and are caused by the resonance in the air cavity of the MPP absorber. If the height of source and receiver position is increased gradually, then the dips will shift to lower frequencies due to the interference effect caused above the surface of the micro-perforated panel. Generally, a significant dip will appear at lowest frequencies.

Second, there are sharp dips that are caused by effect of interference on the surface of the micro-perforated panel. In this condition, it can draw sound attenuation at high frequencies around 800-10,000 Hz depending on the configuration during the testing. As shown in Figure 7-9, the proposed model shows a good agreement with experimental results of different configurations during the testing.

Thus, Figure 7-9 show good agreements between theoretical prediction and experimental results, the proposed impedance model of single layer, double layer and mixed construction MPP absorber may be validated.

3.3.2 Normal Incidence Absorption Coefficient

The normal incidence sound absorption coefficient of materials is usually measured by means of a 2-microphone impedance tube method. A B&K type 4206 two-microphone impedance measurement tube and two specially designed 1/4 inch micrphones B&K type 4187 with preamplifiers are used for measurements. A B&K data acquisition front-end type 2827, an ethernet switch and a standard PC and pulse software are used to capture experimental data for subsequent processing. For the measurement in the low frequency range from 40 Hz to 1600 Hz, a larger impedance tube with inner diameter of 100 mm was used; whilst the 29 mm inner diameter smaller tube was used for measurement in the high frequency range from 100 Hz to 6400 Hz.

For the impedance tube measurement, the parameters of MPP absorber were diameter: d = 0.2 mm; thickness of MPP: t = 0.2 mm; distance between the holes: b = 2.3mm; and air cavity: D = 18 mm. Also, the mixed construction absorber, the parameters were flow resistivity: σ = 9 kPa s m^{-2}; thickness of fiberglass: D_f = 200 mm; and density: ρ_1 = 48 kg/m^3 and the parameters of the MPP were diameter: d = 0.3 mm; thickness of MPP: t = 0.15 mm; distance between the holes: b = 3mm. The experimental set-up of these absorbers are shown in Chapter 2 (Figure 6).

The normal absorption coefficient of MPP absorber and mixed construction (MPP with fiberglass) absorber is evaluated based on the proposed model. The experimental results are obtained by impedance tube measurement. Figure 11 indicates that the proposed theory shows good agreement with the experimental results.

The absorption coefficient of MPP absorber as a function of frequencies is shown in Figure 10. In Figure 10, the measured frequency range is 100Hz to 6400Hz and the absorption coefficient is increased with the frequencies until 1500Hz. The absorption coefficient is increased from 0.5 to 0.9 at the frequency range 800Hz and 1500Hz, and then it is decreased to 0.5 until at 2800Hz. The useful frequency range of MPP absorber with thickness 1.8cm is 800Hz and 2800Hz.

Also, the absorption coefficient of mixed construction absorber as a function of frequencies is shown in Figure 11. For impedance tube measurement method, the measured frequency range is 100Hz to 6400Hz. In Figure 11, the absorption coefficient is increased with the frequencies. The absorption coefficient is increased from 0.5 to 0.9 at the frequency range 100Hz and 800Hz. In fact, the useful frequency range of mixed construction absorber with thickness 200mm is 100Hz and 3000Hz. As shown in Figure 10 and Figure 11, the proposed model shows a good agreement with experimental results of MPP and mixed construction MPP absorber. Actually, it is necessary to

substitute the parameter of flow resistivity into the outdoor sound theory to obtain the absorption coefficient of mixed construction absorber against frequencies.

3.3.3 Absorption Coefficient for Random Incidence

The numerical integration for the average absorption coefficient of the single layer MPP absorber was calculated by using a Matlab program. The absorption coefficient of the absorbers was obtained by numerical summation of sound energy for random incidence of sound waves. This is defined as the ratio of the total sound energy absorbed to the total sound energy incidence. In Figure 12, it is shown that the sound absorption coefficient of the MPP absorber for random incidence of sound waves was against frequencies. The parameters of the MPP absorber were diameter: d = 0.4 mm, thickness of MPP: t = 0.4 mm, distance between the holes: b = 7 mm and spacing of air cavity: D = 50 mm.

According Liu *et al.*[7], the reverberation room measurements have been carried out in a laboratory at Beijing acoustics research center. The measurement is based on the assumption that the sound field in the reverberation room is diffuse. In this experiement, the sound absorption measurement included the principles and testing proceduces is depended on international acoustic standard of ISO 354 -1985. The size of reverberation room is 190 m^3 and the surface area is 9 m^2. In the reverberation room measurement, the measured frequency range was up to 5000Hz. These measurements have also been conducted by Liu *et al.*[7] and refer to this Figure 6. The experimental result of micro-perforated panel (MPP) absorber has no edge effect, and can be useful for further verifying the numerical evaluation of sound energy absorption of MPP absorber based on the proposed theory. The comparison between the calculated and measured absorption coefficients of a single layer of the absorber is shown in Figure 12. The agreement between the calculation and measurement is very reasonable. Thus, the

proposed theory can model the absorption performance of the MPP absorber. Based on the Eq. (21), the variation of direct sound wave distance and spherical reflected sound waves situation may be analysed. As shown in Figure 13, the average absorption coefficient would be shift to lower frequencies when receiver is closer to the sound source. Since the sound diffusion for random incidence is not enough if the receiver is much closer, the absorption performance of MPP absorber is like normal incidence condition. In Figure 13, the distance of direct sound waves are 100m, 50m, 5m and the range of source height is 1m to 3m. Therefore, the limitation of receiver position may be determined based on the proposed formula. Also, this formula is more applicable and useful for design of the sound absorber position.

3.4 Discussion

Determination of sound fields due to a point source over the MPP absorber is achieved based on the proposed model in this chapter. The present model is based on outdoor sound propagation theory and the Maa's theory. As shown in Figures 7-9, the sound attenuation due to interference effect over the MPP absorber is determined at different configuration. Figure 7 and Figure 8 indicate that the incident angle of sound waves on the surface of single and double MPP absorber is 64.5° and 44.5° respectively. The theoretical prediction shows a good agreement with the experimental result. Thus, the oblique acoustic impedance of MPP absorber based on Maa's theory may be validated and become more rigorous. In our validation work, we can fully understand the oblique acoustic impedance of MPP absorber and it is very useful for practical purpose because sound waves propagate with different angles of incidence in realistic situation very often. Also, Figures 9 show that the sound fields over the mixed MPP absorber may be predictable. The agreements between the calculated values and measurement data are very reasonable. Moreover, the absorption performance of mixed

construction (MPP with fiberglass) absorber is studied. If the MPP absorber is combined with fibrous material such as fiberglass, the sound absorption performance will be improved especially in lower frequencies. Therefore, we propose this type of sound absorbers can be used as low frequency absorber for industrial application and it can eliminate the noise generated from machine, such as fan, pump, chiller unit, etc. Consequently, the sound attenuation over the mixed construction absorber and energy absorption coefficient of the absorber may be determined. The proposed formula is established to evaluate the average absorption coefficient for random incidence of sound waves. It makes us more understand the variation of absorption performance of sound absorber which depend on the distance between source and receiver.

As shown in Figure 12, the proposed theory can be well modeled the angle-averaged absorption coefficient in the reverberation room because the edge effect is eliminated in this case. Normally, edge effect is also known as diffraction effect. The apparent boost in sound absorption coefficient that comes about due to wave diffraction at the edges of the specimen. The specimen appears to be larger than its plan area. Thus, the effect is most noticeable when values exceed 1.0 and most low-frequency results for highly absorptive specimens are affected to some degree. The MPP absorber is a sound resonator system and it is not an absorptive material so the absorption performance is not affected by edge effect.

3.5 Conclusions

Based on the above studies, the sound fields due to a point source over the micro-perforated panel (MPP) absorber has been firstly determined. Compared with experimental results, the proposed theory shows good agreement. Secondly, the numerical prediction of angle-averaged absorption coefficient based on the proposed theory is evaluated using Matlab program. The agreements between prediction and

published data are very reasonable. Since the proposed theory can provide detail information of sound absorption of MPP absorbers of different configuration, it can be used for design optimisation of MPP absorber for environmental noise absorption applications. The present study also improves our understanding of the sound absorption performance of MPP absorber. For future research work, we propose micro-perforated panel absorber can be used in outdoor environment as well as interior spaces. Therefore, a site measurement can be conducted in order to realise the sound attenuation and absorption based on our proposed theory for further investigation.

References

(1) Maa, D.Y. "Design and the theoretical study of micro-perforated panel construction". *China academy of science*, pp.245-257, (1975)

(2) Maa, D.Y. "Microperforated panel wideband absorbers". *Noise control engineering journal*, Nov.-Dec. (1987)

(3) Maa, D.Y. "Design of microperforated panel constructions". *Acta Acustica*, Vol. 13 No.3, (1988)

(4) Maa, D.Y. "Potential of microperforated panel absorber". *Journal of the Acoustical Society of America*, Vol. 104 No.5, (1998)

(5) Zhang, Z.M. and Gu, X.Y. "The theoretical and application study on a double layer microperforated sound absorption structure". *Journal of sound and vibration*, Vol. 215 No.3, pp.399-405 (1998)

(6) Kang, J. and Fuchs, H.V. "Predicting the absorption of open weave textiles and micro-perforated membranes backed by an air space". *Journal of sound and vibration*, Vol. 220 No.5, pp.905-920 (1999)

(7) Liu, K. , Nocke, C. and Maa, D.Y. "Experimental investigation on sound absorber characteristic of micro-perforated panel in diffuse fields". *Acta Acustica*, Vol. 25 No.3 (2000)

(8) Deleny, M.E. and Bazley, E.N. "Acoustical properties of fibrous absorbent materials". *Applied Acoustics*, p.3 (1970)

(9) Li, K.M. , Fuller, T.W., and Attenborough, K. "Sound propagation from a point source over extended-reaction ground". *Journal of the Acoustical Society of America*, Vol. 104 No.2, August (1998)

Figures

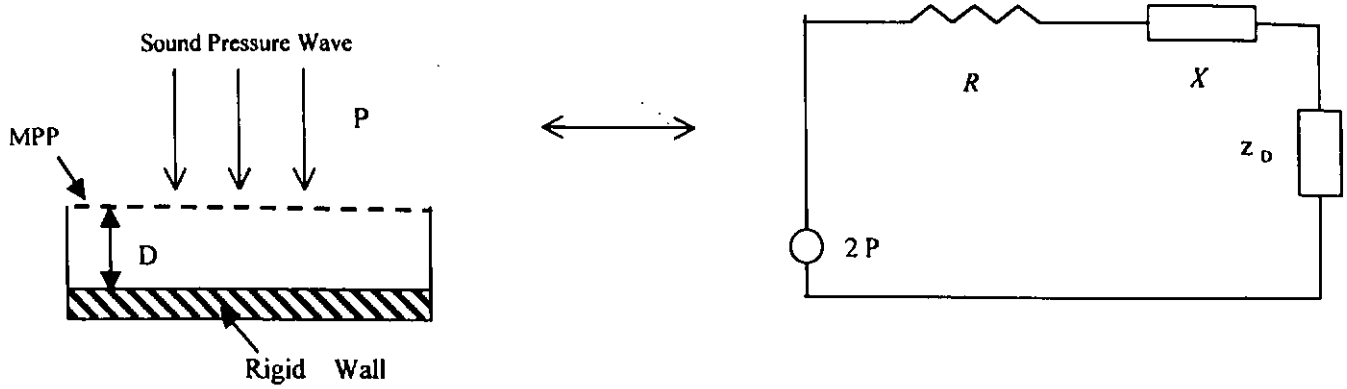

Figure 1 For single layer of MPP absorber: The acoustic impedance of each element of the whole resonant system may be obtained by electric analogous to the open-circuit voltage.

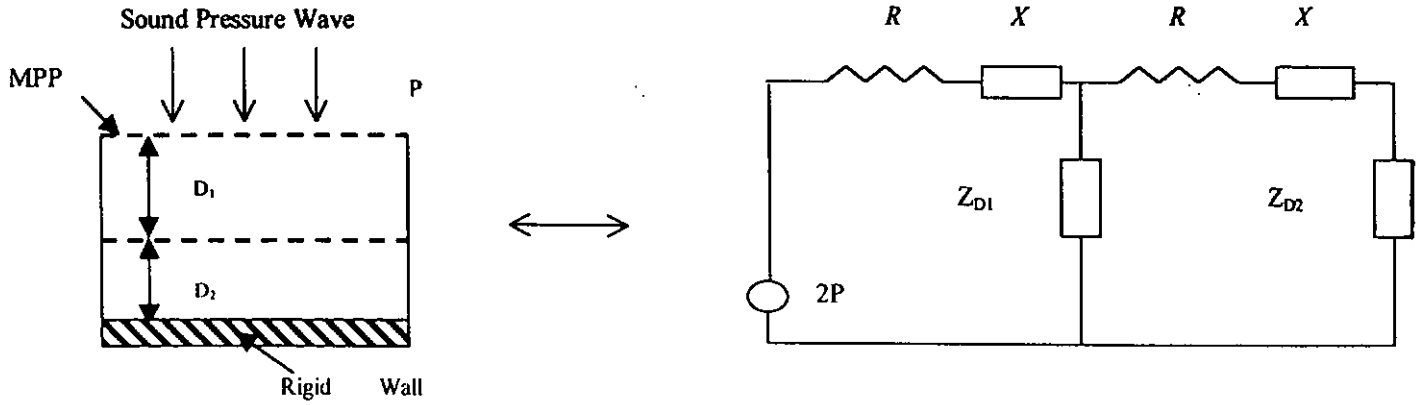

Figure 2 For double layer of MPP absorber: The acoustic impedance of each element of the whole resonant system may be obtained by electric analogous to the open-circuit voltage.

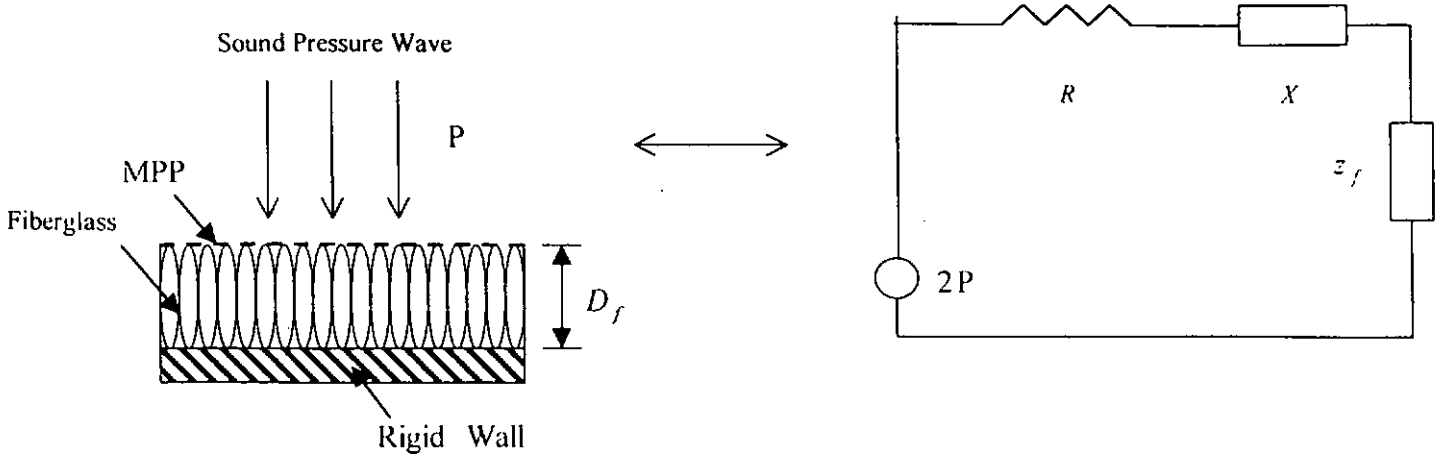

Figure 3 For mixed construction (MPP with fiberglass) absorber: The acoustic impedance of each element of the whole resonant system may be obtained by electric analogous to the open-circuit voltage.

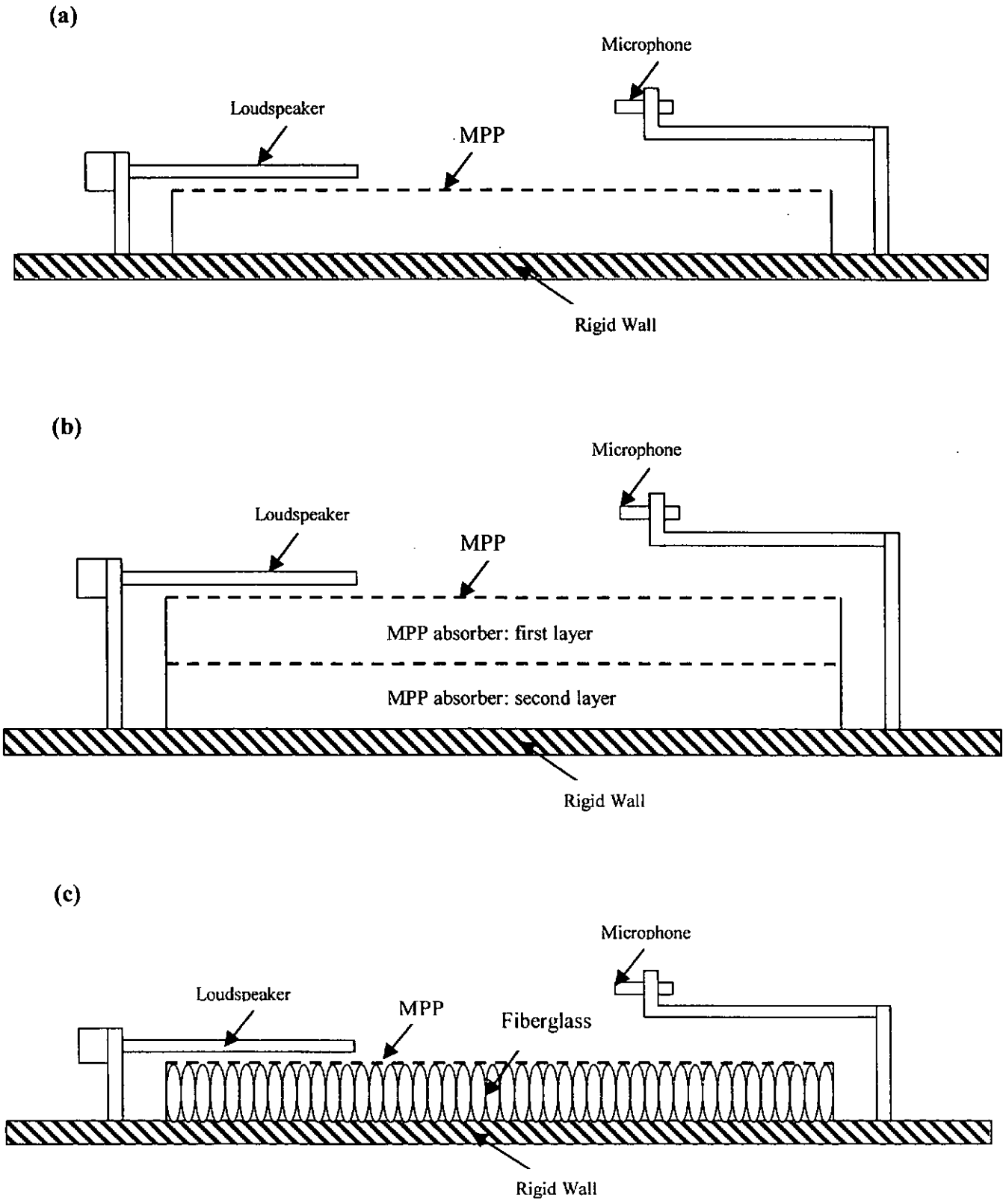

Figure 4 Schematic diagram of the experimental setup,
(a) A single layer of MPP absorber.
(b) A double layer of MPP absorber.
(c) A micro-perforated panel laid on top of fiberglass.

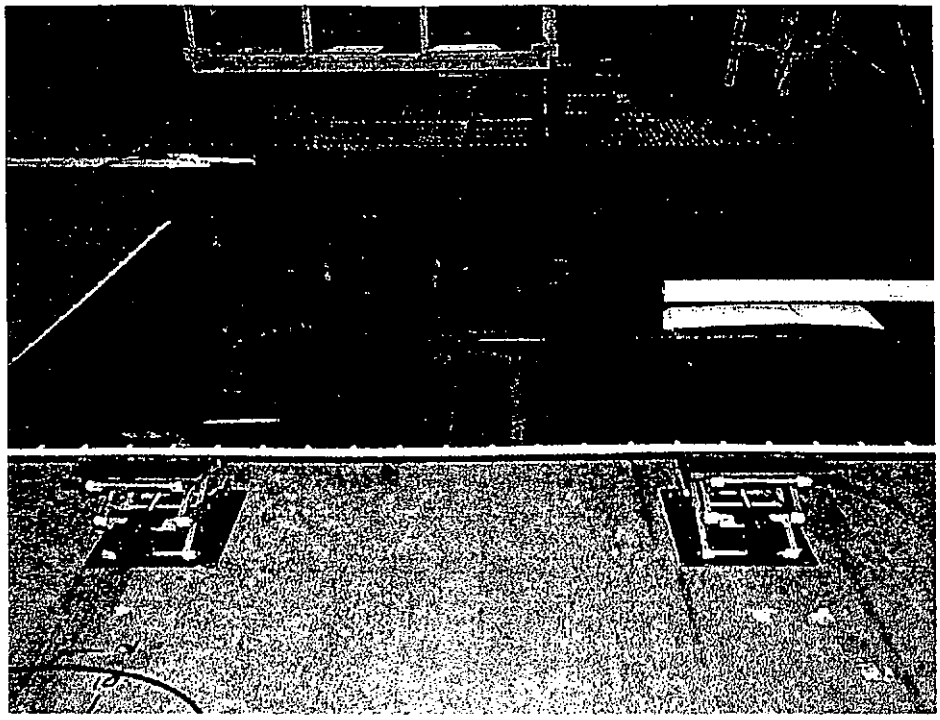

Figure 5 Experimental setup of single layer MPP absorber inside anechoic chamber

Figure 6 Experimental setup of double layer MPP absorber inside anechoic chamber

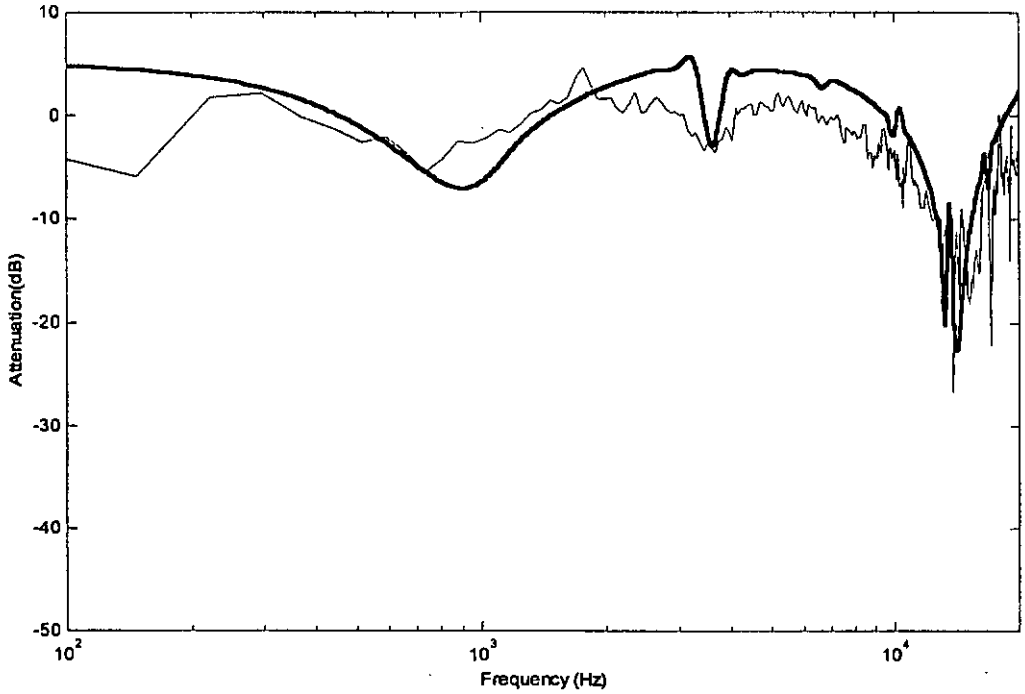

Figure 7 For single layer micro-perforated panel (MPP) absorber: Attenuation data obtained with source height = 1.7cm, receiver height = 17.4 cm, range = 40cm and angle of incidence = 64.5°. Parameters: r=40cm, d=0.3mm, b=3mm, t=0.15mm and D= 12cm
Experimental result (solid line) and theoretical result (thick solid line)

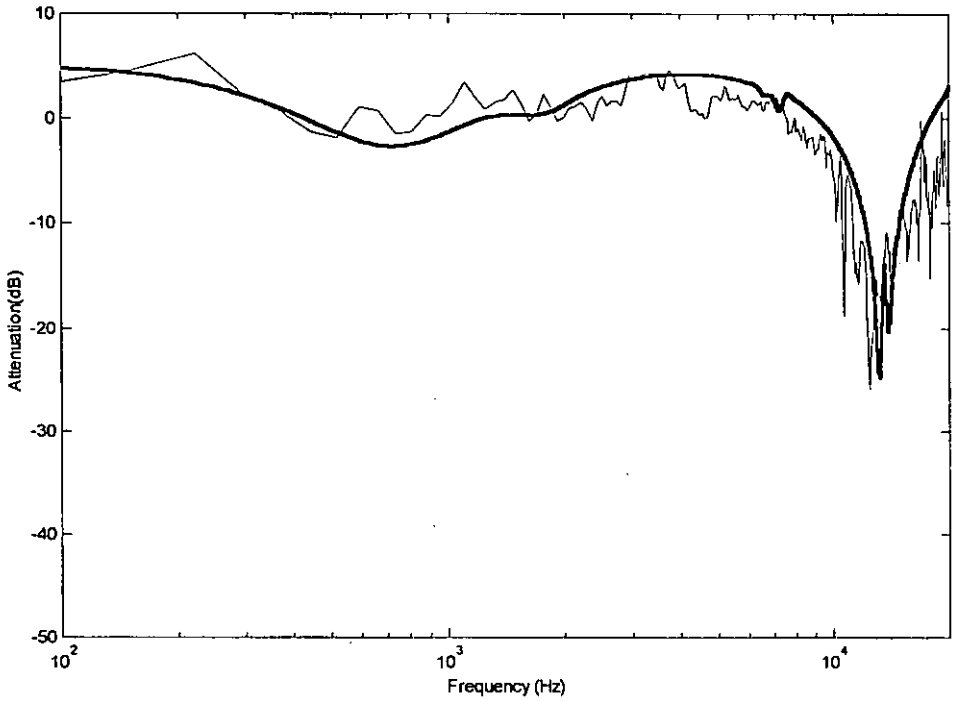

Figure 8 For double layer micro-perforated panel (MPP) absorber: Attenuation data obtained with source height = 1.7cm, receiver height = 22.3 cm, range = 50cm and angle of incidence = 64.4°. Parameters: r=50cm, d=0.3mm, b=3mm, t=0.15mm, D_1=6cm and D_2=6cm
Experimental result (solid line) and theoretical result (thick solid line)

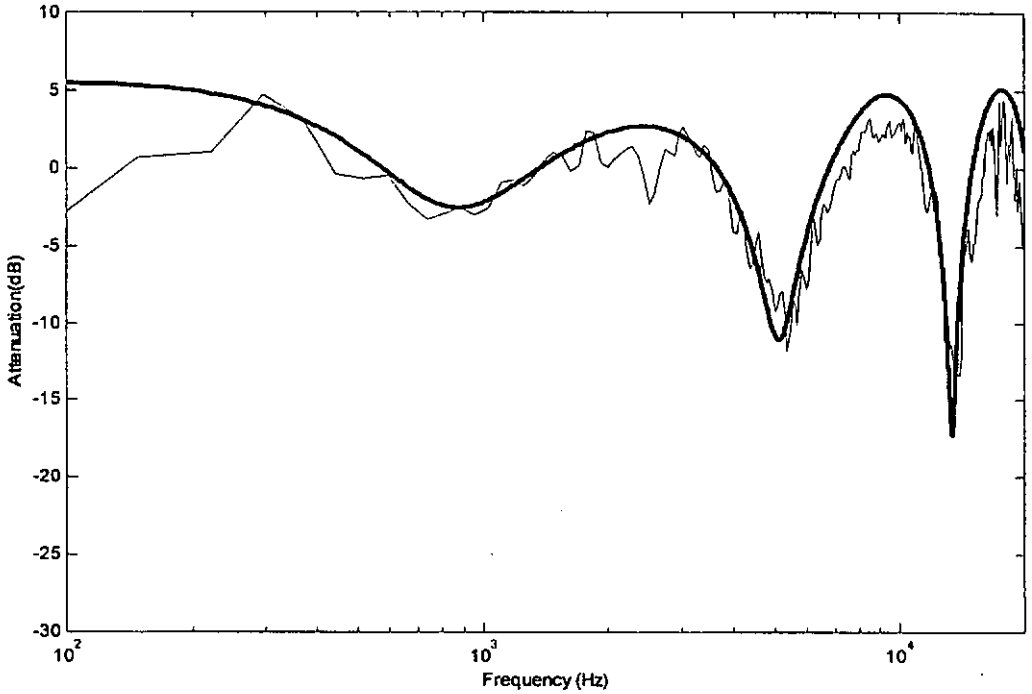

Figure 9 For micro-perforated panel with fiberglass(mixed construction) absorber: Attenuation data obtained with source height = 5.5cm, receiver height = 23.5 cm, range = 60cm, angle of incidence = 64.2°. Parameters: r=60cm, d=0.3mm, b=3mm, t=0.15mm
Experimental result (solid line) and theoretical result (thick solid line)

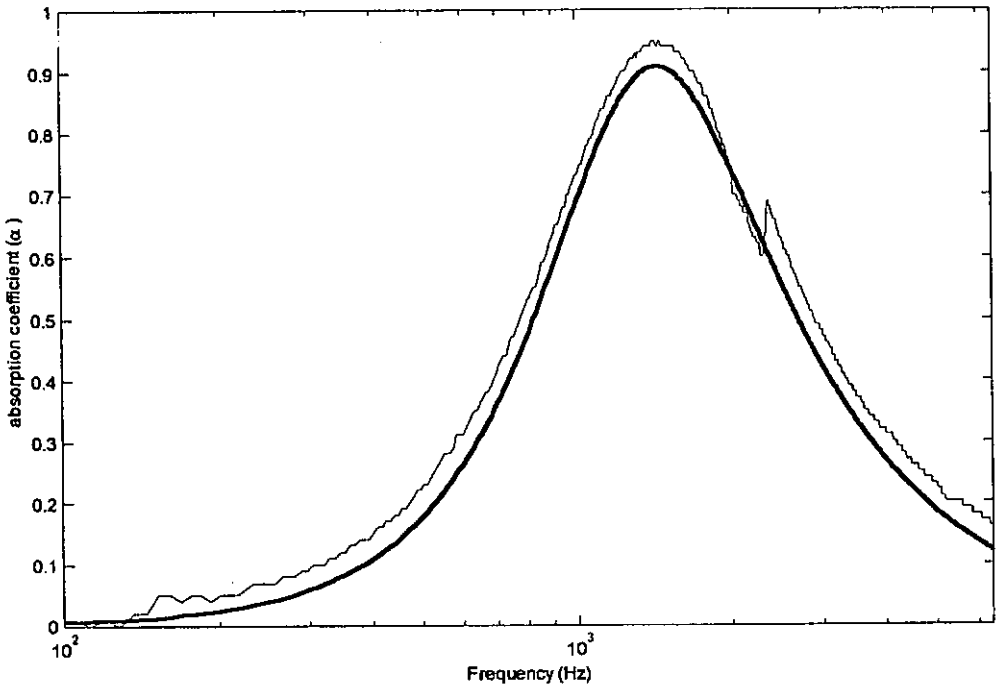

Figure 10 Absorption coefficient of MPP absorber for small impedance tube measurement. Parameter of the absorber is d=0.2mm, t=0.2mm, b=2.3mm and D =18mm Experimental result (solid line) and theoretical result (thick solid line).

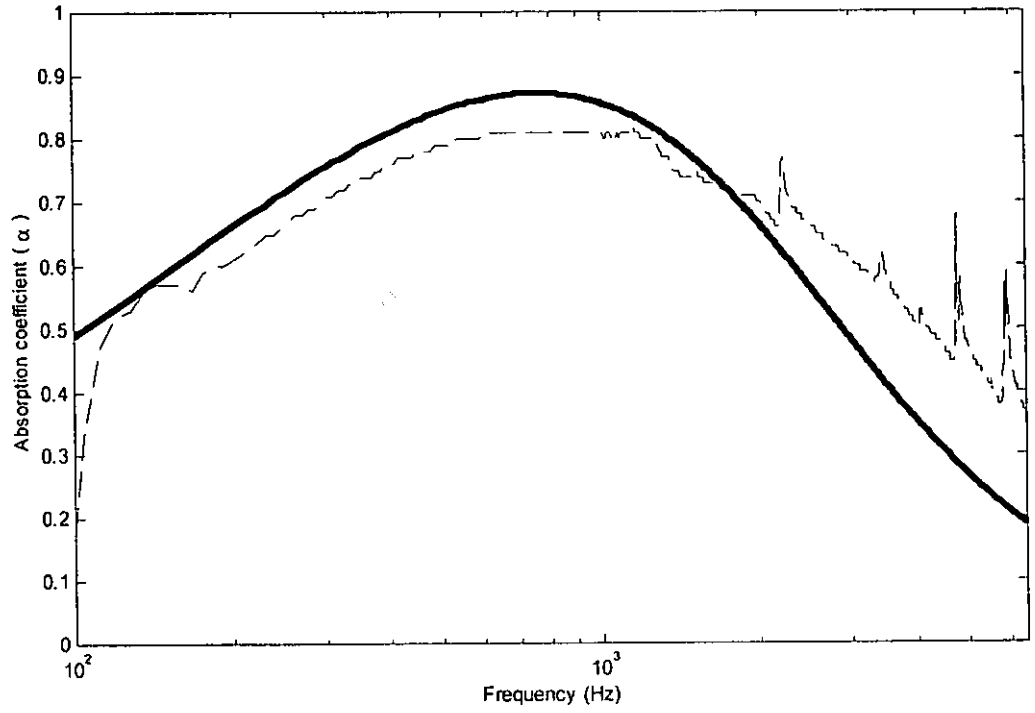

Figure 11 Absorption coefficient of MPP with fiberglass absorber for small impedance tube measurement. Parameter of the absorber is d=0.3mm, t=0.15mm, b=3mm. Experimental result (solid line) and theoretical result by semi-infinite model (thick solid line).

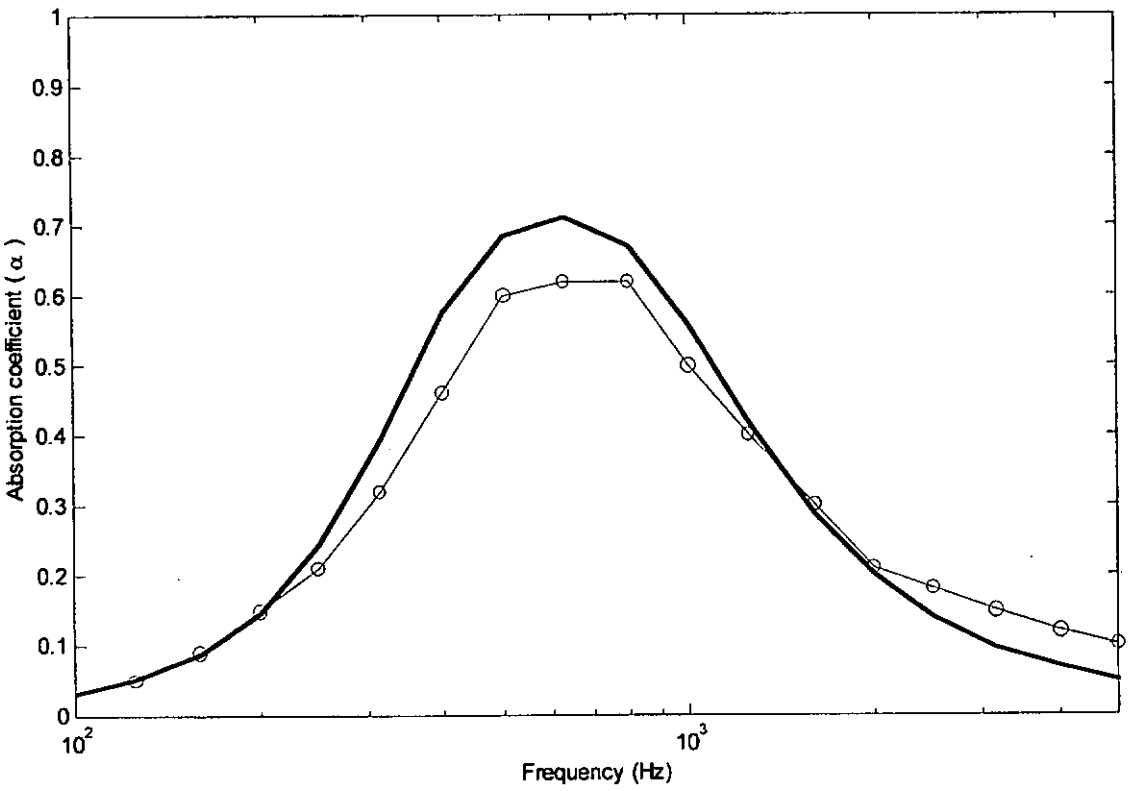

Figure 12 Absorption coefficient of single layer MPP absorber for random incidence of sound waves.

Parameter of the absorber is d=0.4mm, t=0.4mm, b=7mm, D = 50mm

Experimental result (solid-circle line) and theoretical result (thick solid line).

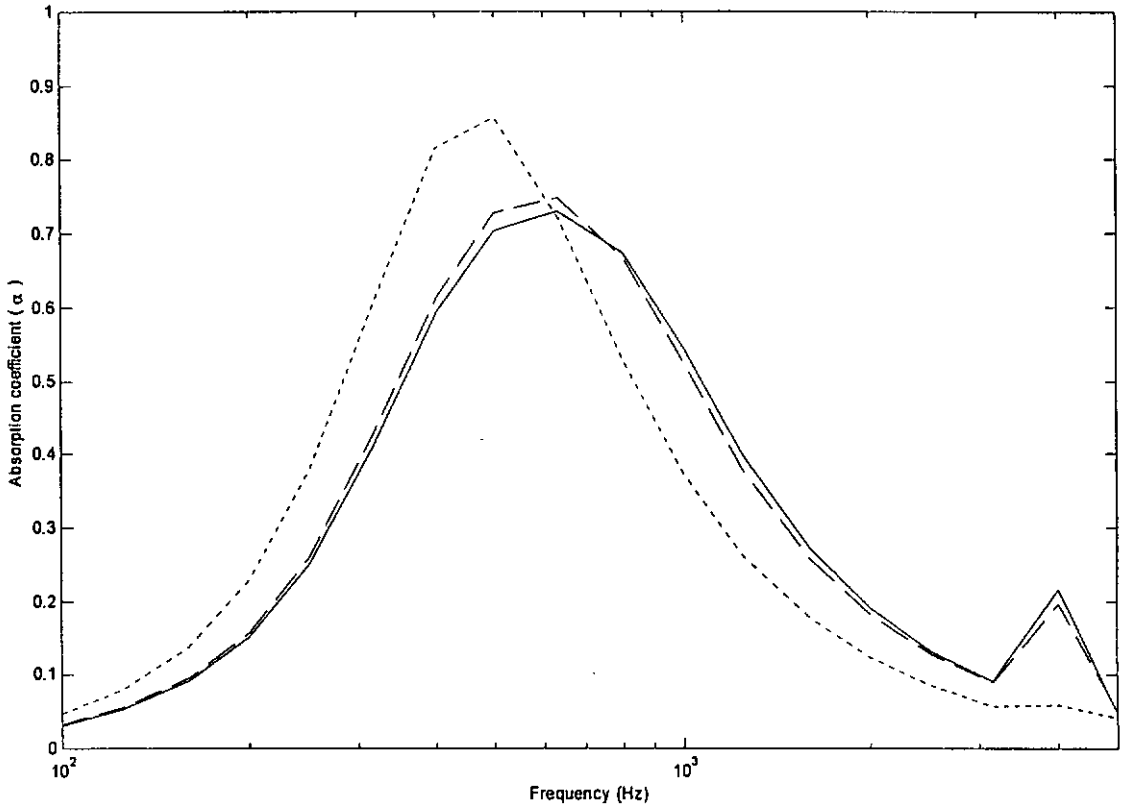

Figure 13 Absorption coefficient of single layer MPP absorber for random incidence of sound waves.

Parameter of the absorber is d=0.4mm, t=0.4mm, b=7mm, D = 50mm

Theoretical result (solid line) where r_1 = 100m and $1<h_s<3$.
Theoretical result (dashed line) where r_1 = 50m and $1<h_s<3$.
Theoretical result (dot line) where r_1 = 5m and $1<h_s<3$.

CHAPTER 4

Theoretical Model of Perforated Facings on Sound Absorption Materials

4.1 Introduction

On the basis of previous studies in Chapter 3, the sound fields due to a point source over a single layer MPP absorber, a double layer MPP absorber and a mixed construction (MPP with fiberglass) absorber is determined. Also the absorption performance of the MPP absorbers is obtained based on the proposed theory. Thus, the derivation of the oblique acoustic impedance of the MPP absorber based on Maa's theory should be more rigorous. The first objective of this chapter is to extend the proposed theory for further analysis and apply the theory on the sound absorption materials covered with perforated facings. Secondly, the impedance model of the absorption material with perforated facings is determined and the numerical evaluation for absorption coefficient of the absorber is presented. Thirdly, in order to consolidate the present model, an equivalent electrical circuit approach (EECA) and a boundary element method (BEM) is used to verify the proposed theory.

Bolt[1] developed an approximate analysis of the absorption characteristic of sound absorption materials with perforated facings. He provided engineering design charts for acoustic treatment based on his analysis. Ingard and Bolt[2] extended the analysis of the sound absorption performance of absorption materials with perforated facings. The approximate analysis included the combination of a perforated facing and thin layer absorption material with or without air cavity, and the absorption performance of the absorber in detail. Afterwards, Ingard[3] indicated that the acoustic impedance of

perforated facing usually contributes mass reactance to the total impedance. It is shown that the facing also causes an additional acoustic resistance, which is often larger than the acoustic resistance of the fiberglass layer alone. The resistance can be obtained when the absorption is in close contact with the facing.

In the relevant literature, most researchers reported investigation of the normal absorption coefficient of sound absorption materials with perforated facings. In recent years, Philippe Guignouard *et al.*[4] proposed an impedance model to evaluate the absorption performance of the fiberglass materials with perforated facings for oblique incidence of sound waves. Also, Takahashi[5] attempted to predict the average absorption coefficient of a periodical arranged flat surface. However, the excess absorption clearly occurred due to edge effect in the frequency range from 125Hz to 4000Hz. It was found that the flow resistivity of the fiberglass material was related to the degree of excess absorption at medium and high frequencies. The thickness of the rigidly backed fiberglass layer was related to the absorption at low frequencies. Thus, Takahashi[6] developed a model that includes the effect of the diffraction phenomenon caused by impedance discontinuities of the boundary surface. However, the numerical results based on his model still did not agree well with his experimental data.

Sound absorption materials covered with perforated facings are commonly used in architectural acoustics and noise control problems. Thus, a reliable method for predicting the performance of the absorber is required. Lee and Chen[7] developed a simple and accurate analytical acoustic transmission analysis for predicting absorption coefficient of the multi-layer sound absorber. The numerical results based on the transmission analytical model have been compared with an equivalent electrical circuit approach (EECA). The EECA developed by Jinkyo *et al.*[8] is one of the most popular approaches. In this approach, the sound pressure, particle velocity and acoustic

impedance are respectively analogous to the voltage, electrical current and acoustic impedance. Therefore, the absorption coefficient of sound absorber is obtained by using the resultant acoustic impedance of the absorber.

Furthermore, many researchers[11-13] have developed the appropriate theory for predicting the sound fields over an impedance discontinuity boundary. In recent years, a reliable theoretical method is required for predicting the sound fields over a mixed impedance ground or surface. Chandler-Wilde and Hothersall[14] developed boundary element method for predicting the sound fields due to a point source over an inhomogeneous normally reacting flat ground. The boundary element method modeled the sound propagation was effectively two-dimensional. Similarly, Habault[15] indicated that the boundary element method was convenient for evaluation of the sound fields over an inhomogeneous plane. However, the numerical method of computation of the sound fields above an inhomogeneous plane did not provide a correct prediction if each part of the plane was not accurately described by the boundary condition chosen. Afterwards, Harriott *et al.*[16] proposed an improved calculation method based on boundary element method for sound propagation over an inhomogeneous impedance ground. It may save computation time and is an approximate method for predicting the sound fields over the inhomogeneous impedance ground.

Patrice Boulanger *et al.*[17] published that comparison between experimental measurements and models of sound propagation due to a point source over mixed impedance ground. The theoretical models include De Jong, Nyberg's theory, a Fresnel-zone approximation and boundary element method. Compared with the models, boundary element technique performs a good agreement with the measurements. Thus, boundary element technique is a reliable method to predict the sound fields due to a point source over a mixed impedance ground or surface. Also, Patrice Boulanger *et al.*[18]

attempted to compare with experimental results of sound propagation over hard rough surface by their analytical proposed theory and boundary element method. The method was used to predict sound propagation over surface containing 2-D roughness of any shape. As a result, the boundary element technique performed even better prediction than their proposed model.

In the present study, the impedance model of the perforated facings on sound absorption materials and the absorption coefficient of the absorber based on the proposed theory are presented. The numerical predictions of average absorption coefficient based on the proposed theory show a good agreement with the corresponding EECA analysis result. Indoor laboratory measurements of absorption coefficient have been carried out in a reverberation room. Also, the sound attenuation of the absorption materials with perforated facings absorber based on boundary element method is determined. The absorber may simulate a mixed impedance surface of perforated plate and fiberglass. Comparison of the results based on our proposed theory and the boundary element technique will be presented. The numerical integral results are obtained in order to compare with the proposed theory for verification. In literature surveys, boundary element method is generally used for solving problems of 2-D mixed impedance surface or ground. Thus, a 3-D approximate boundary element method is derived to perform a realistic situation. Reasonable agreements between numerical prediction and experimental results are obtained. This model is an alternative theoretical method for predicting the sound fields and absorption performance of the perforated facings on absorption materials absorber. Although the average absorption coefficient due to edge effect has not been considered, this method is simple and it is a useful design tool for outdoor and indoor environment.

4.2 Review of the Equivalent Electrical Circuit Approach

4.2.1 *Acoustics Impedance of Perforated facings on Sound Absorption Material*

In acoustic system analysis, the equivalent electrical circuit approach (EECA) is a popular method to evaluate the total acoustic impedance of the sound absorbers. In this approach, the acoustic pressures, particle velocity and acoustic impedance respectively analogous to the voltage, electrical current and electrical impedance. Jinkyo *et al.*[8] applied the approach to evaluate the total acoustic impedance of sound absorber and obtain the absorption coefficient based on EECA. The acoustic impedance of perforated plate and fibrous material may be simulated and described below:

$$z_p = \frac{\rho_o}{\varepsilon}\sqrt{8\nu\omega}\left(1+\frac{t_p}{2r}\right)+i\frac{\omega\rho_o}{\varepsilon}\left[\sqrt{\frac{8}{\omega}}\left(1+\frac{t_p}{2r}\right)+t_p+\delta\right] \quad (1)$$

where z_p is the acoustic impedance of perforated plate, ρ_o is the air density, ν is the kinematic viscosity of air (ν=15 x 10^{-6} m^2/s) at room temperature, ω is the angular frequency and $i = \sqrt{-1}$. t_p , r , ε $(=\pi r^2/b^2)$ and δ $(=0.85(2r)f(\varepsilon))$ are the thickness, hole radius, porosity and viscous boundary layer thickness of the perforated plate respectively. b is the hole pitch of the perforated plate and $f(\varepsilon) = 1-1.47\sqrt{\varepsilon}+0.47\sqrt{\varepsilon^3}$.

For homogeneous and isotropic porous materials, the acoustic impedance of fibrous material may be determined based on a report of Delany and Bazley[9]. The empirical power law relationship for the complex wave propagation constant γ and specific acoustic impedance Z_m may be expressed as:

$$\gamma = 10.3\frac{\omega}{c_o}\left(\frac{f}{\sigma}\right)^{-0.59}+\frac{\omega}{c_o}\left[1+10.8\left(\frac{f}{\sigma}\right)^{-0.7}\right] \quad (2)$$

and

$$Z_m = 1 + 9.08\left(\frac{f}{\sigma}\right)^{-0.75} - 11.9\left(\frac{f}{\sigma}\right)^{-0.73} \tag{3}$$

Hence, if the fibrous material is backed by rigid wall, the surface acoustic impedance may be expressed as

$$z_m = Z_m \coth(\gamma t_m) \tag{4}$$

where f is the sound frequency, σ is the flow resistivity and t_m is the thickness of the fibrous material. Thus, the total specific acoustic impedance z_T of perforated facings on fibrous material may be expressed as:

$$z_T = \frac{z_p}{\rho_o c_o} + z_m \tag{5}$$

4.2.2 *Evaluation of Normal and Average Absorption Coefficient*

The acoustic absorption coefficient of fibrous material covered with perforated facings can be obtained from the above resultant total acoustic impedance. The normal α_n and oblique absorption coefficient α_θ may be evaluated based on the following equation.

$$\alpha_n = 1 - \left|\frac{z_T - 1}{z_T + 1}\right|^2 \tag{6}$$

and

$$\alpha_\theta = 1 - \left|\frac{z_T \cos\theta - 1}{z_T \cos\theta + 1}\right|^2 \tag{7}$$

In a diffuse sound field, the angle-averaged absorption coefficient α_{AV} can be obtained from

$$\alpha_{AV} = 2\int_0^{\pi/2} \alpha_\theta \sin\theta \cos\theta \, d\theta \tag{8}$$

where θ is the angles of incidence of sound waves.

4.3 Theoretical model of the Impedance of Perforated facings on Sound Absorption Material

The sound absorber with perforated facings on fibrous materials was made as a metal sheet with many holes of diameter greater than 1mm backed by a fibrous material. As shown in Figure 1, it can be shown that the acoustic impedance of each element of the whole resonant system may be obtained by electrical analogue.

The normal acoustic impedance of the perforated panel absorber is

$$Z_{perforated} = R + iX + Z_f \tag{9}$$

Also the oblique acoustic impedance of the perforated panel absorber can be written as

$$Z_{perforated\vartheta} = R\cos\theta + iX\cos\theta + Z_f \tag{10}$$

where R and X are the real and imaginary parts of the normalized specific acoustic impedance of the perforated facings and Z_f is the normalized specific acoustic impedance of the fiberglass.

4.4 Testing results

4.4.1 Experimental results

To confirm the validity of the impedance model for perforated facings on fiberglass absorbers, numerical predictions based on the proposed model was compared with experimental results. The experimental data are obtained by using (i) a standard impedance tube and (ii) indoor standard ground characterization measurements by MLSSA system. Those results have also been compared with the relevant experimental

results reported by researchers who conducted experiments in a standard reverberant chamber.

Experimental testing of perforated facings on fibrous materials absorber was carried out in the anechoic chamber of the Mechanical Engineering Department of The Hong Kong Polytechnic University. The sound attenuation of the absorber was measured by the maximum length sequence (MLS) system based on the principle of maximum length sequence system analyzers (MLSSA). The perforated facing panel was made of stainless steel. The fibrous material of sample 1 (pink) was tested and the parameters of the sample 1 fiberglass absorber were: density, ρ_1 = 48kg/m^3; and thickness of fiberglass, D_f = 50mm. The parameters of the perforated facings were: diameter, d = 2.5 mm; pitch, b = 5 mm; and thickness, t = 0.6 mm.

The sound fields due to a point source over the perforated facings on fibrous material was determined inside the anechoic chamber of size 6 × 6 × 3 m (high). A Tannoy driver with a tube of 3 cm internal diameter and 1 m long was used as a point source in this experiment. The sound source was connected to a maximum length sequence system analyzer (MLSSA) with an MLS card installed in a PC. The analyzer was connected to a B&K 2713 amplifier. The MLSSA system was used both as the signal generator for the source and as the signal-processing analyzer. A BSWA TECH MK224 1/2 inch condenser microphone and a BSWA TECH MA201 preamplifier were used together as the receiver. Both source and receiver were placed at a fixed position by means of a stand and clamps. The range between the source and receiver was fixed with only their heights adjusted for different sets of measurement.

In these experiments, the sound attenuation above the absorbers was measured in various configurations. During the experiments, the source and receiver were placed above and to each side of sample 1 with perforated facing absorber of height 10cm. The

distance between the source and receiver was 1m. The experimental set-up of the absorber is shown as Figure 2.

4.4.2 *Numerical Simulation Results*

The sound attenuation over the perforated facings on fiberglass absorber was obtained based on the proposed model. Also, the numerical computational results were evaluated using the Matlab program. In order to verify the proposed theory, outdoor sound experimental measurement was conducted in the anechoic chamber. The experimental results of perforated facings on sample 1 were shown in Figure 3.

As seen in Figure 3, the sound attenuation due to a point source over sample 1 with perforated facing absorber was determined. The distance between the sound source and the surface of the absorber was 10cm. The range between the position of source and receiver was 1m. In Figure 3, a significant dip appears at particular frequency which depended on the configuration. It draws about 6 dB at 800 Hz and the attenuation frequency range is 300Hz to 3000Hz. Thus, the frequency bandwidth is 2700Hz. Also, the flow resistivity of sample 1 is 15000 Pa s m^{-2} .

The experimental results show good agreement with the proposed theory. The sound attenuation of the perforated facings on fiberglass absorbers can be ascertained by subsituting the acoustic impedance of oblique incidence into Weyl van der Po formula of the outdoor sound theory. As a result, the proposed model can be used to determine the sound fields due to a point source over sample 1 on perforated facings absorber with certain configuration. Also, the proposed theoretical method may predict sound attenuation of the perforated facings on fiberglass absorber with different flow resistivities.

4.5 Boundary Element Method (BEM)

For numerical verification of the proposed theory, boundary element method developed by Chandler-Wilde and Hothersall[14] is presented to predict sound field over a flat inhomogeneous impedance surface. In this chapter, boundary element method, existing 2-D approximate boundary element method and 3-D approximate boundary element method are introduced to verify the sound attenuation over perforated facings on fiberglass absorber. Thus, fibrous material covered with perforated facings is simulated as an inhomogeneous impedance plane[14].

For boundary element method, the mathematical expression of this problem as a two-dimensional boundary values problem, which is shown below[14]:

$$p(t_1,t_2) = G_{\beta_2}(t_1,t_2) + ik(\beta_1 - \beta_2)\int_{-\infty}^{\infty} p(s,t_1)G_{\beta_2}(s,t_2)dx \tag{11}$$

where $t_1 = (0, H_s)$ is the source position, $t_2 = (r, H_r)$ is the receiver postion, β_1 and β_2 are the admittances of the boundary. Also $s = (x,0)$ is a point in the boundary. For two points t_1 and t_2, $p(t_1,t_2)$ denotes the acoustic potential detected by a receiver at t_2 when insonified by a unit source at t_1, and $G_\beta(t_1,t_2)$ denotes the same quantity in the simple case when the boudary has homogeneous admittance β, where $\beta = \beta_1$ or β_2.

Thus, the sound attenuation over the perforated facings on fiberglass absorber

$$= 20\log\left|\frac{p_{perforaed}}{\frac{e^{ikr}}{4\pi r}}\right| \tag{12}$$

where r is horizontal distance between sound source and receiver, $p_{perforated}$ is $p(t_1,t_2)$.

4.5.1 2-D Approximate BEM

Also, Harriott *et al.*[16] proposed an approximate method for saving computation

time and is an existing 2-D approximate boundary element method. In this case, $p(s,t_1)$ in Eq. (11) is replaced by $G_{\beta_1}(s,t_1)$, so the approximation equation is shown below[16]:

$$p_A(t_1,t_2) = G_{\beta_2}(t_1,t_2) + i(\beta_1 - \beta_2)I(X) \tag{13}$$

where $I(X) = k\int_{-\infty}^{X} G_{\beta_1}(s,t_1)G_{\beta_2}(s,t_2)dx$ and p_A is the acoustic potential over the inhomogeneous impedance plane.

Thus, the sound attenuation over the perforated facings on fiberglass absorber

$$= 20\log\left|\frac{p_{perforaed}}{\frac{e^{ikr}}{4\pi r}}\right| \tag{14}$$

where r is horizontal distance between sound source and receiver, $p_{perforated}$ is $p_A(t_1,t_2)$.

4.5.2 3-D Approximate BEM

The problem of 3-D approximate boundary element technique is shown in Figure 4. Sound attenuation due to a point source over a flat surface of fibrous material with perforated facings is determined. A point source is located above the inhomogeneous impedance plane and the plane is divided into many rectangular regions to form a boundary impedance plane. The mathematical expression of 3-D boundary integral equations are derived below:

Using Eq. (13) above, the 3-D approximate boundary integral equation may be written as:

$$p_{3D,A}(t_1,t_2) = G_{\beta_2}(t_1,t_2) + i(\beta_1 - \beta_2)I(X,Y) \tag{15}$$

where $I(X,Y) = k\int_{-\infty}^{Y}\int_{-\infty}^{X} G_{\beta_1}(s,t_1)G_{\beta_2}(s,t_2)dxdy$. To consider a cylinderical source over the rectangluar perforated surface, we have to calculate $Q_A(t_1,t_2)$, an approximate cylinderical wave reflection coefficient. The approximate acoustic potential due to the

cylinderical wave over the impedance surface can be determined and the Eq. (15) may be shown as below:

$$p_{3D,A}(t_1,t_2) = -(i/4)\mathrm{H}_0^{(1)}(kR_1) + Q_A(t_1,t_2)[-(i/4)\mathrm{H}_0^{(1)}(kR_2)] \tag{16}$$

where $\mathrm{H}_0^{(1)}$ is the Hankel function of the first kind of order zero, R_1 and R_2 denote the distances from source and from image source to receiver respectively. Harriott *et al.*[16] indicated that $Q_A(t_1,t_2)$ is an accurate approximation to $Q(t_1,t_2)$, the spherical wave reflection coefficient. Thus, when considering the point source in the 3-D problem, the exact acoustic potential at the receiver position is

$$P_{3D}(t_1,t_2) = -(\mathrm{e}^{ikR_1}/4\pi R_1) - Q(t_1,t_2)(\mathrm{e}^{ikR_2}/4\pi R_2) \tag{17}$$

Replacing $Q(t_1,t_2)$ with $Q_A(t_1,t_2)$, an approximate reflection coefficient. So, the approximate acoustic potential due to a point source over the impedance surface in 3-D problem can be determined and Eq. (17) may be written as:

$$P_{3D,A}(t_1,t_2) = -(\mathrm{e}^{ikR_1}/4\pi R_1) - Q_A(t_1,t_2)(\mathrm{e}^{ikR_2}/4\pi R_2) \tag{18}$$

Thus, the sound attenuation due to a point source over the rectangualr perforated facings on fiberglass absorber in approximate 3-D problem

$$= 20\log\left|\frac{p_{perforaed}}{\frac{e^{ikr}}{4\pi r}}\right| \tag{19}$$

where r is the horizontal distance between sound source and receiver, $p_{perforated}$ is $P_{3D,A}(t_1,\mathrm{t}_2)$.

Based on Eq. (15) above, the rectangular perforated surface may be simulated as an approached circular perforated surface. The diagram of this 3-D problem in circular perforated surface situation is shown in Figure 5. The accuracy of numerical integration depends on the element size in x and y-axes.

4.6 Numerical Verification for the Proposed Model

The sound attenuation due to a point source over the fibrous material with perforated facings is determined based on the proposed theory. In order to verify the proposed theory, boundary element method, 2-D approximate boundary method and 3-D approximate boundary element method are used to generate results for comparison. In general, those methods are very accurate to predict the sound fields over impedance surface and are based on boundary integral equations. The sound attenuation over the fibrous material covered with perforated facings as a function of frequencies is shown in Figure 6(a)-(c).

As shown in Figure 6(a), the proposed model illustrates that it draws sound attenuation of 5.5dB at 1,100Hz. Also, the useful frequency range is 600Hz to 2,000Hz. Compared to proposed model, 2-D boundary element method shows that the sound attenuation is 4.5dB at 1,100Hz. Thus, the difference of sound attenuation is about 1dB. When the certain frequencies exceed 2,000Hz, it is observed that the difference of sound attenuation is still 1dB. The agreement of both proposed model and 2-D BEM is reasonable.

As shown in Figure 6(b), the proposed model illustrates that it also draws maximum sound attenuation of 5.5dB at 1,100Hz. Compared with the proposed theory, 2-D approximate boundary element method shows that the maximum sound attenuation is 4.5dB at 1,400Hz. Thus, the difference of sound attenuation and frequency is about 1dB and 300Hz. When the certain frequencies exceed 2,000Hz, it is observed that the difference of sound attenuation is about 1dB. The agreement of both proposed theory and 2-D approximate BEM shows fairly good.

As seen in Figure 6(c), the proposed model illustrates that it draws maximum sound attenuation of 5.5dB at 1,100Hz. Compared with the proposed model, 3-D

approximate boundary element method shows that the maximum sound attenuation is 5.5dB at 1,200Hz. Thus, the difference of sound attenuation and frequency is about 0dB and 100Hz. When the certain frequencies exceed 2,000Hz, it is observed that the difference of sound attenuation is still 0.05dB. Thus, both the proposed model and 3-D approximate BEM shows very reasonable agreement. To sum up the above numerical results, the proposed theory agrees well with the 3-dimensional approximate boundary element prediction as depicted in Figure 6(c) while it shows reasonable agreement with the 2-dimensional boundary element theory and 2-D approximate solution theory as shown in Figure 6(a) and Figure 6(b) respectively.

Also, the sound attenuation determined by 3-dimensional boundary element method in circular shape is shown in Figure 6(d). In Figure 6(d), a significant dip appears at 1,000Hz and it draws sound attenuation about 6dB. The practical interest of frequency range is 600Hz to 2,000Hz. The numerical prediction shows very good agreement with our proposed theory. Compared with 3-dimensional boundary element method in rectangular shape, the agreements between both numerical results are quite reasonable because the diameter of the holes is not very large. The parameter of the sound absorber of diameter is 5.8mm, thickness is 1mm, pitch is 7mm and thickness of fibrous material is 50mm. Thus, the deviation of 3-dimensional boundary element method with circular and rectangular elements is small. Figure 6(d) indicates that the 3-dimensional boundary element model with rectangular elements is good enough to verify our proposed theory in this case.

4.7 Absorption Performance of Perforated Facings on Fibrous Materials

4.7.1 Normal absorption coefficient

The two-microphone impedance tube was used to measure the sound absorption coefficient of the sample 1 with perforated facings absorbers. The apparatuses of this experiment are the B&K two-microphone impedance measurement tube type 4206, power amplifier type 2706, two specially designed 1/4 inch micrphones type 4187 with preamplifiers, data acquisition front-end type 2827, ethernet switch, a standard PC and pulse softtware. For the measurement in the low frequency range (40Hz-1,600Hz), a large impedance tube with inner diameter of 100mm was used; whilst the 29mm inner diameter small tube was used for measurement in the high frequency range (160Hz-6,400Hz).

For the impedance tube measurement, the measured frequency range was up to 6.4 kHz. For the perforated panel absorber, the parameters of the absorber were diameter: d = 2.5 mm; thickness of perforated panel: t = 0.6 mm; and distance between the holes: b = 5mm. The fiberglass of sample 1 had flow resistivity: σ = 15 kPa s m^{-2} and thickness of fiberglass: D_f = 50 mm. The experimental set-up of the absorber is shown in Figure 6 of Chapter 2.

4.7.2 Numerical Results

Absorption coefficient of the perforated facings on fiberglass absorbers was evaluated numerically by a Matlab program. To obtain the absorption coefficient of the perforated facings on fiberglass absorbers against frequencies, it is necessary to substitute the best-fit parameter of flow resistivity into the outdoor sound propagation theory. In Figure 7, it can be seen that the experimental results of two microphones impedance tube

method show good agreement with the theoretical prediction based on the proposed theory.

The normal absorption coefficient of sample 1 with perforated facing absorber as a function of frequencies is shown in Figure 7. As seen in Figure 7, it is shown that the measured frequency range is up to 6,400Hz for small impedance tube measurement. Figure 7 observes that the absorption coefficient of sample 1 with perforated facing is about 1.0 at 1,500Hz and maintain the absorption performance up to 6,400Hz. The absorption coefficient is about 1 at certain frequencies (1500Hz and 3500Hz). Thus the useful frequency range for practical use is 1,500Hz to 6,400Hz. It is quite significant for sound absorption at the high frequency range. As a result, it can be concluded that the proposed theory shows good agreement with the experimental results of sound attenuation and the absorption coefficient on the absorbers.

4.7.3 Average absorption coefficient

Reverberation room measurements have been carried out in a laboratory at Switzerland. The measurement is based on the assumption that the sound field in the reverberation room is diffused. In this experiement, the principles and testing procedure of sound absorption measurement follow the international acoustic standard ISO 354 - 1985. One type of fiberglass was tested. The parameters of sample 1 (pink) fiberglass absorbers are density: ρ_1 = 48kg/m^3; and thickness of fiberglass: D_f = 50mm. For perforated facings, the parameters are diameter: d = 2.5mm, distance between adjacent holes: b = 5mm and thickness of the perforated facings: t = 0.6mm. The size of reverberation room is 211 m^3 and the surface area is 12 m^2. Also, the temperature and relative humidity of the room is 20°C and 60% respectively.

4.7.4 *Numerical Results*

The numerical integration of the average absorption coefficient on the fiberglass with perforated facing absorber was evaluated using the Matlab program. The absorption coefficient of the absorbers was obtained by numerical summation of sound energy for random incidence of sound waves. This is defined as the ratio of the total sound energy absorbed to the total sound energy incidence. Figure 8 indicate that the sound absorption performance of the perforated facings on sample 1 fiberglass absorbers for random incidence of sound waves versus sound frequencies. For the fiberglass sample, the flow resistivity was 15000 Pa s m^{-2} and the thickness is 50 mm. Also, the parameters of the perforated facing were: d = 2.5 mm, b = 5 mm, t = 0.6 mm and D_f = 50 mm.

As shown in Figure 8, the average absorption coefficient of sample 1 is a function of sound frequency. The measured frequency range is up to 5,000Hz. It is shown that the trend of the numerical prediction for average absorption coefficient is very similar to the experimental results. Thus the absorption coefficient obtained experimentally is typically greater than 1 at wide frequency range because of edge effect. Figure 8 shows that absorption coefficient at 600Hz starts to exceed 1 up to 2,000Hz. The deviation of absorption coefficient between experimental results and numerical prediction is large and the difference of absorption coefficient is about 0.2. However, when absorption coefficient is increased to 2,000Hz, the absorption performance of sample 1 is declined. The absorption coefficient of the sample is decreased to about 0.8 and the deviation of experimental results and numerical prediction is about 0.1 until 5,000Hz.

4.7.5 *Comparison of the Proposed Theory and the Equivalent Electrical Circuit Approach (EECA)*

The normal and average absorption coefficients are evaluated based on the equivalent electrical circuit approach (EECA) using the Matlab program. Compared with the EECA, numerical result of normal absorption based on the proposed theory shows a good agreement. The normal absorption coefficient of sample 1 fiberglass with perforated facings as a function of frequencies is shown in Figure 9. Very reasonable agreements between the EECA and the proposed method can be observed. The normal absorption coefficient increases with frequencies until 1,000 Hz from 0.1 to 0.99. Also, the normal absorption coefficient maintains almost constant until 6,400 Hz. The practical useful frequency range 300 Hz to 6,400 Hz covers absorption coefficient above 0.5. The difference of absorption coefficient based on proposed theory, EECA and experimental measurement is about 0.01.

Compared to the EECA, numerical result of average absorption based on the proposed theory shows a good agreement. The average absorption coefficient of sample 1 fiberglass with perforated facings as a function of frequencies is shown in Figure 10. The predictions by both the EECA and the proposed model are reasonably matched. The average absorption coefficient is increased with frequencies until 600 Hz from 0.1 to 0.8. Also, the average absorption coefficient keeps constant up to 3,000 Hz. However the absorption coefficient is slightly decreased with frequencies about 0.1 above 3000Hz because the sample 1 fiberglass is covered with the perforated facings. The practical useful frequency range 300 Hz to 5000 Hz covers absorption coefficient above 0.5. The difference of absorption coefficient based on proposed theory and EECA is about 0.03.

4.8 Discussion

The sound fields due to a point source over perforated facings on sound absorption materials are determined based on the proposed model. As shown in Figure 3, a significant dip appears at the lowest frequency and several sharp dips appear at high frequencies. Compared with fiberglass absorbers, a significant dip still appears due to inference effect above the absorber but no sharp dip would appear at high frequencies. A sharp dip appears at high frequencies because the effect of interference above the hard surface of the non-perforated part. Thus, the phenomena of sound attenuation over the sound absorption materials covered perforated facings absorber is very similar to sound absorption materials absorber. The perforated facings are commonly used for protection use only. So the perforated facings on sound absorption materials absorbers may be more suitable used in outdoor environment.

The sound fields due to a point source over the fiberglass with perforated facings absorber is determined based on the proposed method and boundary element method. Compared with the proposed method, the numerical results of boundary element method show good agreements. However, there are constraints in both the proposed method and the boundary element method.

In fact, the boundary element method is generally solving 2-dimensional problem and typically concerned about the sound fields over a finite boundary condition. The sound fields over a homogeneous or an inhomogeneous ground may be determined accurately. It is a realistic model for predicting the sound fields over an impedance surface with different shapes. The coordinates of the impedance surface, the position of source and receiver have to be located exactly. However, the computation time for evaluating the sound fields based on boundary element technique is very long. Especially for high frequencies, the computation time would be very long due to the element size is

small. Normally, the element size is equal to or smaller than the wavelength of sound. Thus, the numerical results of boundary element method are not accurate when the element size is not small enough.

For the proposed model, it concerns about the sound fields over an infinite boundary condition and the solution of sound fields may be obtained easily. Thus, computation time based on the proposed theory for evaluating the solution of sound fields would be shorter and faster than the boundary element method. However, the proposed theory just modeled a fixed shape of impedance surface and may not simulate a real case situation.

Boundary element method is a 2-dimensional (2-D) problem so we have to consider a 3-dimensional (3-D) situation to approach the proposed model. As shown in Figure 6(a)-(c), the 3-D approximate boundary element method provide the best agreement with the proposed theory because the proposed model is applied for sound fields over an infinite homogeneous or inhomogeneous impedance surface with 3-D problem. Thus, 3-D approximate boundary element technique is derived and used to compare with the proposed model very well.

The normal absorption coefficient of the perforated facings on sound absorption materials absorber is presented. The agreements between the calculated values and experimental data are very reasonable. The absorption performance of the absorber is typically at high frequencies. The practical useful frequency bandwidth is between 1,000Hz and 6,400Hz. Also, the average absorption coefficient of the absorber is obtained numerically and experimentally. As shown in Figure 8, average absorption coefficient of the absorber is normally greater than 1 due to edge effect or area effect. The effect of frequency range covers 100Hz to 5,000Hz. Also, the definition of absorption coefficient is the ratio of the total sound energy absorbed to the total sound energy

incidence. Thus, the experimental results of such seems to be impossible. However, the trend of both numerical prediction and experimental results is very similar. The proposed model shows fair agreement with the experimental results. The model leads to reasonable numerical results in Figure 8. The absorption performance of fiberglass absorber at high frequencies is normally declined if it is covered with a perforated plate and remains constant at low frequencies.

Based on the comparison of both the proposed model and the EECA, it is shown that the proposed theory is a more reliable and general for predicting sound absorption performance of sound absorbers. The limitation of EECA is the hole diameter of the perforated plate. The numerical prediction does not show a good agreement with experimental result when the diameter of hole is less than 1mm. The normal absorption coefficient is a function of frequencies as shown in Figure 11. Also, it is observed in Figure 11 that our proposed theory shows a good agreement with the experimental result by impedance tube measurement but the EECA does not. The EECA has not considered the correction factor of air flow friction within the holes so it can not predict the absorption performance of sound absorber with small holes accurately. On the other hand, the proposed theory can predict the absorption performance of sound absorber with small holes of diameter 0.2mm.

4.9 Conclusions

An analytical model for predicting sound fields and the absorption performance over a sound absorber with perforated facing on absorption materials is established. Comparing to similar models reported in literature, it is more general because it includes the sound attenuation due to interference effect above the absorber and absorption coefficient of the absorber.

First of all, boundary element method (BEM) and 2-D approximate method have been tried. The numerical results of those methods are verified experimentally and show fairly agreement with the proposed theory. Secondly, a 3-D approximate BEM is derived, compared with the experimental result and introduced for predicting the sound fields from a point source over an impedance discontinuity surface. The 3-D approximate BEM agrees well with the proposed theory. After the numerical verification based on BEM, it is concluded that the proposed theory may model the sound fields due to a point source over fibrous material covered with perforated facings as well as micro-perforated panel (MPP) absorber. Based on the above discussion, the constraints of both boundary element method and proposed model have been pointed out. It depends mainly on the boundary condition, accuracy and computation time that we have to be considered and concerned.

Compared with the EECA, the proposed theory is more reliable and general because it may predict the absorption performance of perforated facings with fiberglass absorber even if the diameter of hole is less than 1mm. The numerical prediction shows good agreements with the experimental results. Although the numerical evaluation of average absorption coefficient has a bit deviated with experimental results because of edge effect, the numerical prediction shows good agreement with the measurement results and the trend of absorption performance is also quite similar to the experimental results.

References

(1) Bolt, R.H. "On the Design of Perforated Facings for Acoustic Materials". *Journal of the Acoustical Society of America*, Vol. 19(5), (1947)

(2) Ingard, U. and Bolt, R.H. "Absorption Characteristics of Acoustic Material with Perforated Facings". *Journal of the Acoustical Society of America*, Vol. 23(5), (1951)

(3) Ingard, U. "Perforated Facing and Sound Absorption". *Journal of the Acoustical Society of America*, Vol. 26(2), (1954)

(4) Guignouard, P. and Meisser, M. "Prediction and Measurement of the Acoustical Impedance and Absorption Coefficient at Oblique Incidence of Porous Layers with Perforated Facings". *Noise Control Engineering Journal*, May-June (1991)

(5) Takahashi, D. "Excess sound absorption due to periodically arranged absorptive materials". *Journal of the Acoustical Society of America*, Vol. 86 No. 6, (1989)

(6) Takahashi, D. "A new method for predicting the sound absorption of perforated absorber systems". *Applied Acoustics*, Vol. 51 No.1, (1997)

(7) Lee, F.C. and Chen, W.H. "Acoustic transmission analysis of multi-layer absorbers". *Journal of sound and vibration*, Vol. 248(4), pp.621-634 (2001)

(8) Jinkyo, L. , George, W. and Swenson, J. "Compact sound absorbers for low frequencies". *Noise Control Engineering Journal*, Vol. 38, p.109-117 (1992)

(9) Deleny, M.E. and Bazley, E.N. "Acoustical properties of fibrous absorbent materials". *Applied Acoustics*, p.3 (1970)

(10) Li, K.M. , Tim, W.F. and Attenborough, K. "Sound propagation from a point source over extended-reaction ground". *Journal of the Acoustical Society of America*, Vol. 104 No.2, (1998)

(11) Chessell, C.I. "Propagation of noise along a finite impedance boundary". *Journal of the Acoustical Society of America*, Vol. 62(4), pp. 825-834 (1977)

(12) Deleny, M.E. and Bazley, E.N. "Acoustical properties of fibrous absorbent materials". *Applied Acoustics*, p.3 (1970)

(13) Dumin, J. and Bertoni, H.L. "Acoustic propagation over ground having inhomogeneous surface impedance". *Journal of the Acoustical Society of America*, Vol. 70(3), pp. 825-859 (1981)

(14) Wilde, S.N.C and Hothersall, D.C. "Sound propagation above an inhomogeneous impedance plane". *Journal of sound and vibration*, Vol. 98(4),

pp.475-491 (1985)

(15) Habault, D. "Sound propagation above an inhomogeneous plane: Boundary integral equation methods". *Journal of sound and vibration*, Vol. 100(1), pp.55-67 (1985)

(16) Harriott, J.N.B. , Wilde, S.N.C. and Hothersall, D.C. "Long-distance sound propagation over an impedance discontinuity". *Journal of sound and vibration*, Vol. 48(3), pp.365-380 (1991)

(17) Boulanger, P. , Fuller, T.W. , Attenborough, K. and Li, K.M. "Models and measurements of sound propagation from a point source over mixed impedance ground". *Journal of the Acoustical Society of America*, Vol. 102(3), September (1997)

(18) Boulanger, P. , Attenborough, K. , Taherzadeh, S. , Waters-Fuller, T. and Li, K.M. "Ground effect over hard rough surfaces". *Journal of the Acoustical Society of America*, Vol. 104(3), September (1998)

Figures

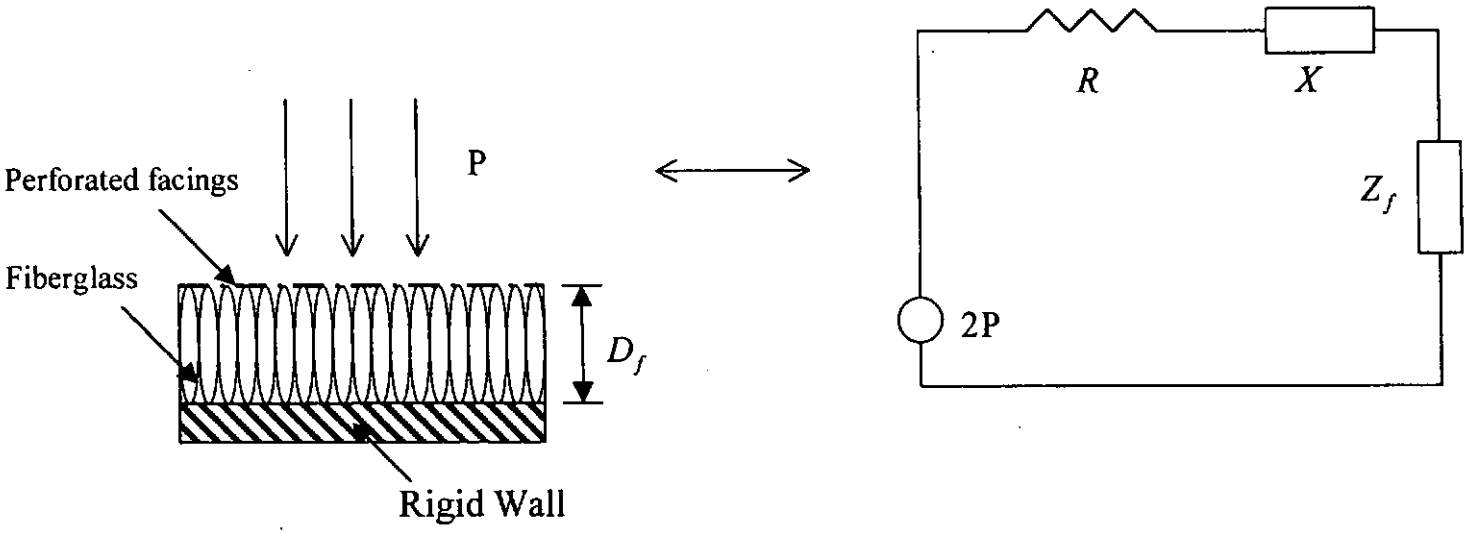

Figure 1 For perforated facings on fiberglass absorber: The acoustic impedance of each element of the whole resonant system may be obtained by electric analogous to the open-circuit voltage.

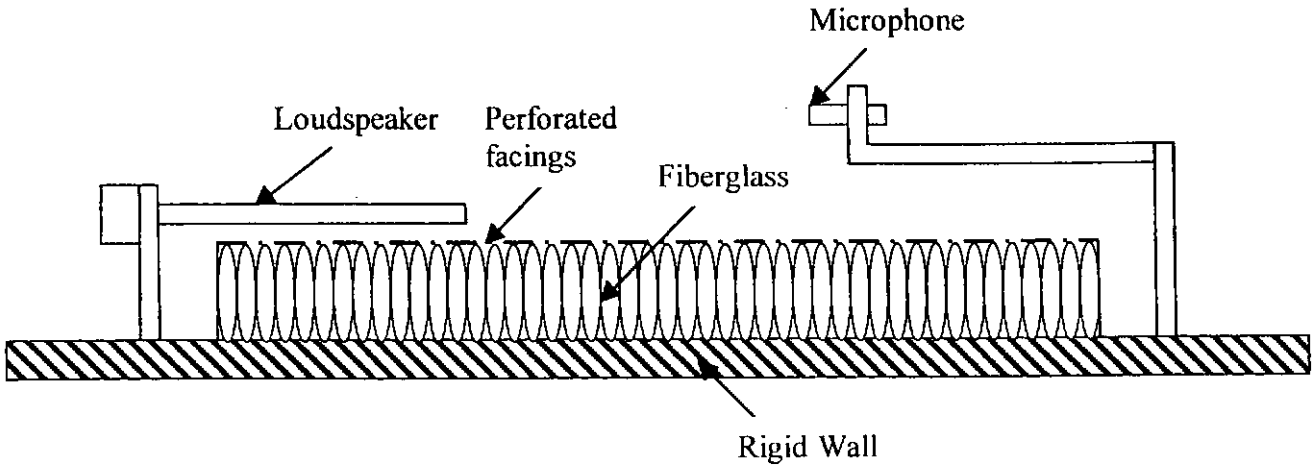

Figure 2 Schematic diagram of the experimental setup of perforated facings on fiberglass absorber.

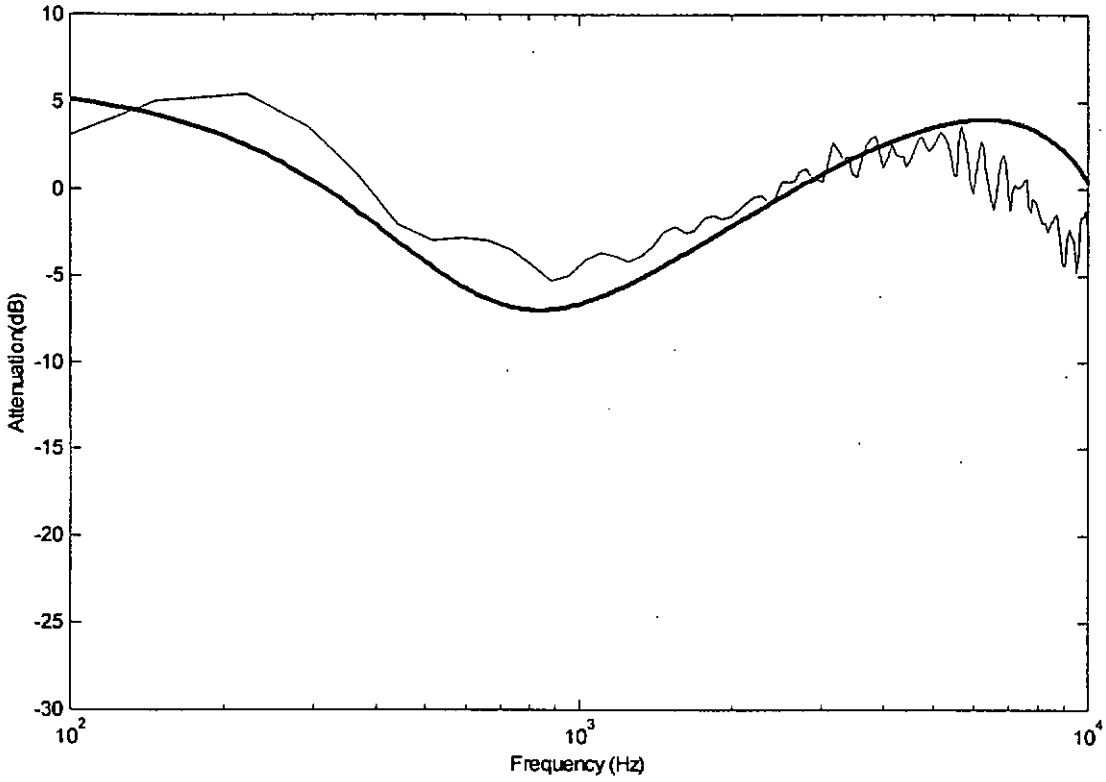

Figure 3 Attenuation data obtained with source height = 10cm, receiver height = 10 cm, range = 1 m and D_f = 50mm.

Parameters: Range=1m, d= 2.5mm, b=5mm and t=0.6mm
Experimental result (solid line) and theoretical result (thick solid line)

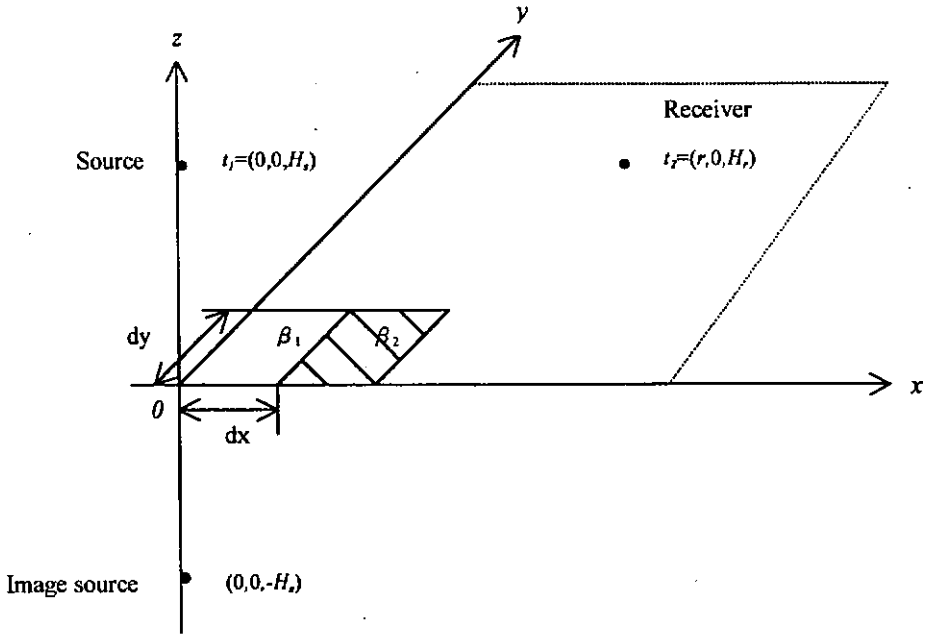

Figure 4 Schematic diagram of 3-D approximate boundary element problem with x and y as the horizontal axes and z as the vertical axis.

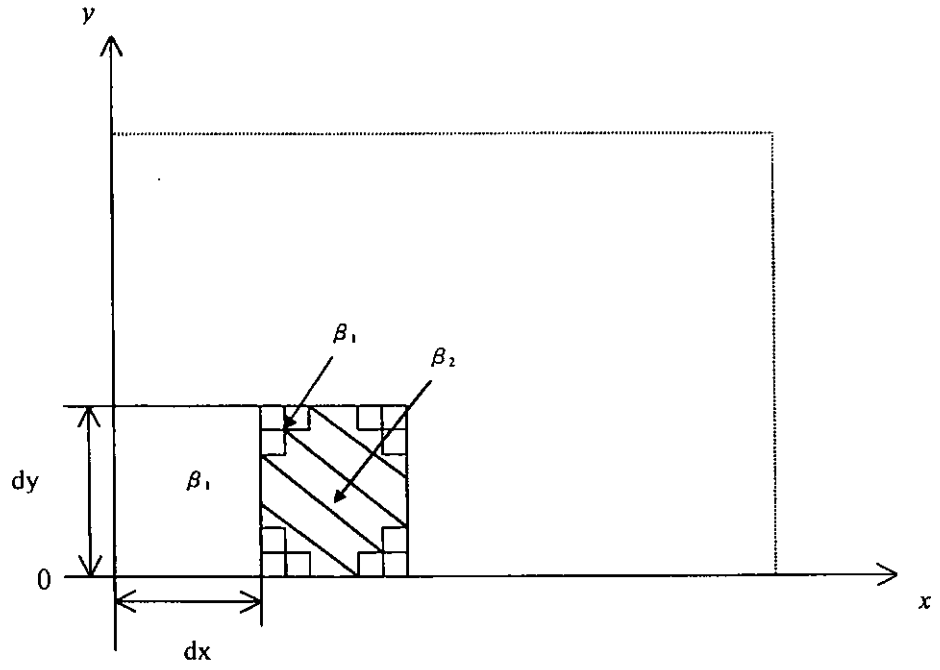

Figure 5 Diagram of 3-D BEM problem in approximate circular perforated surface situation with x and y-axes.

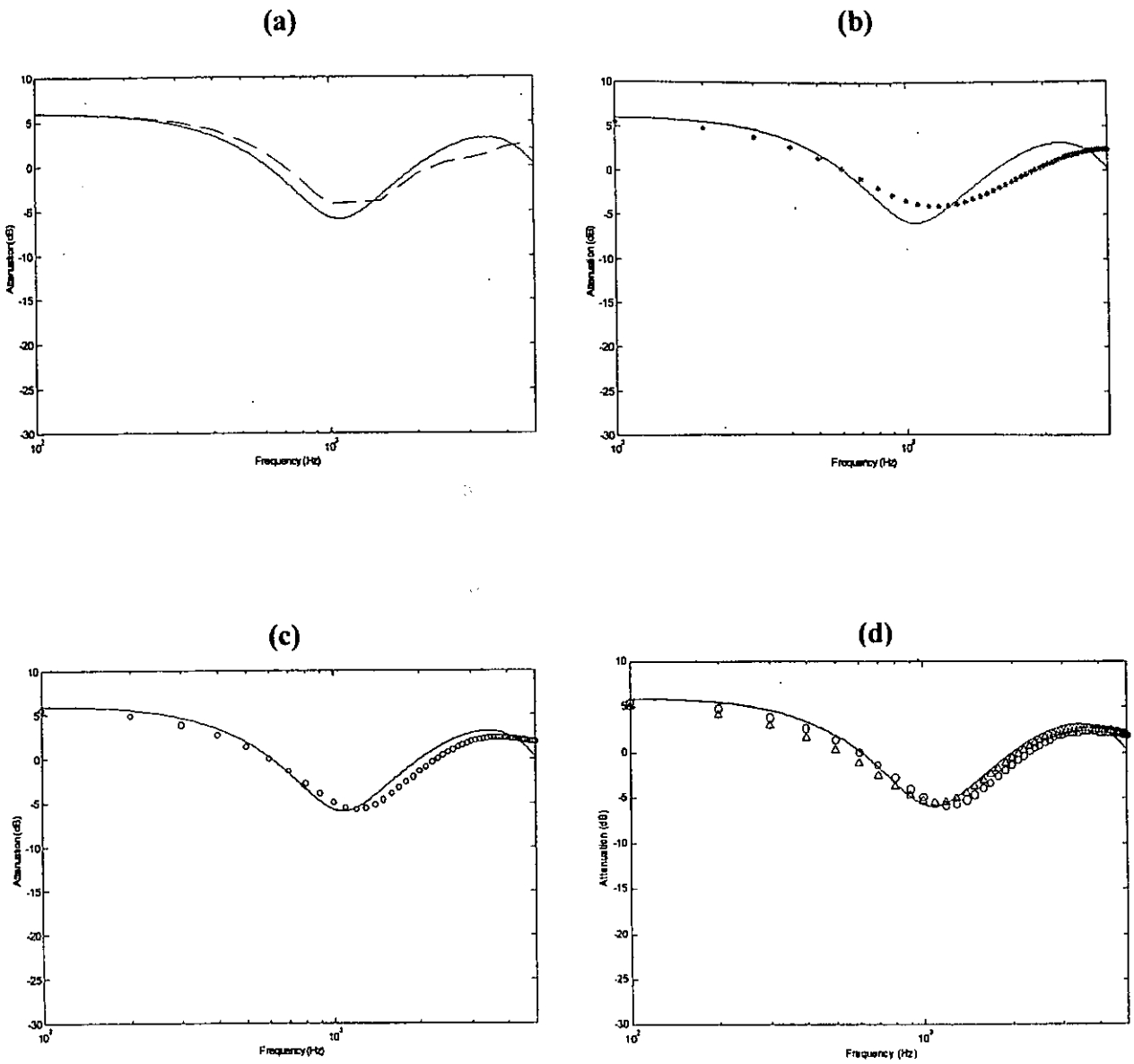

Figure 6 Attenuation data obtained with source height = 0.09m, receiver height = 0.13m and range = 0.6m. Parameter is d = 5.8mm t = 1mm b = 7mm and D_f = 50mm

(a) Theoretical prediction of proposed theory (solid line) and BEM (dashed line)
(b) Theoretical prediction of proposed theory (solid line) and the 2-D approximate BEM (star)
(c) Theoretical prediction of proposed theory (solid line) and the 3-D approximate BEM (circle)
(d) Theoretical prediction of proposed theory (solid line), the 3-D approximate BEM in rectangular shape (circle) and the 3-D approximate BEM in circular shape (triangular)

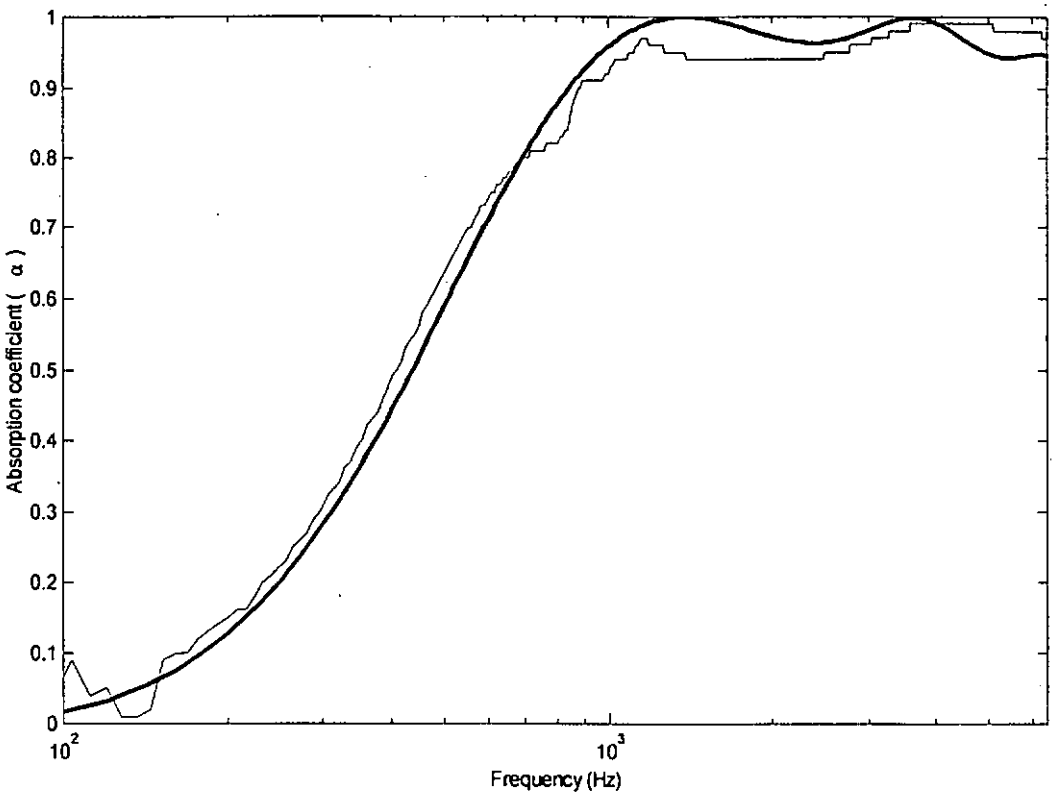

Figure 7 Absorption coefficient of perforated facings on sample 1 fiberglass absorber against different frequencies.
Experimental result (solid line) and theoretical result (thick solid line).

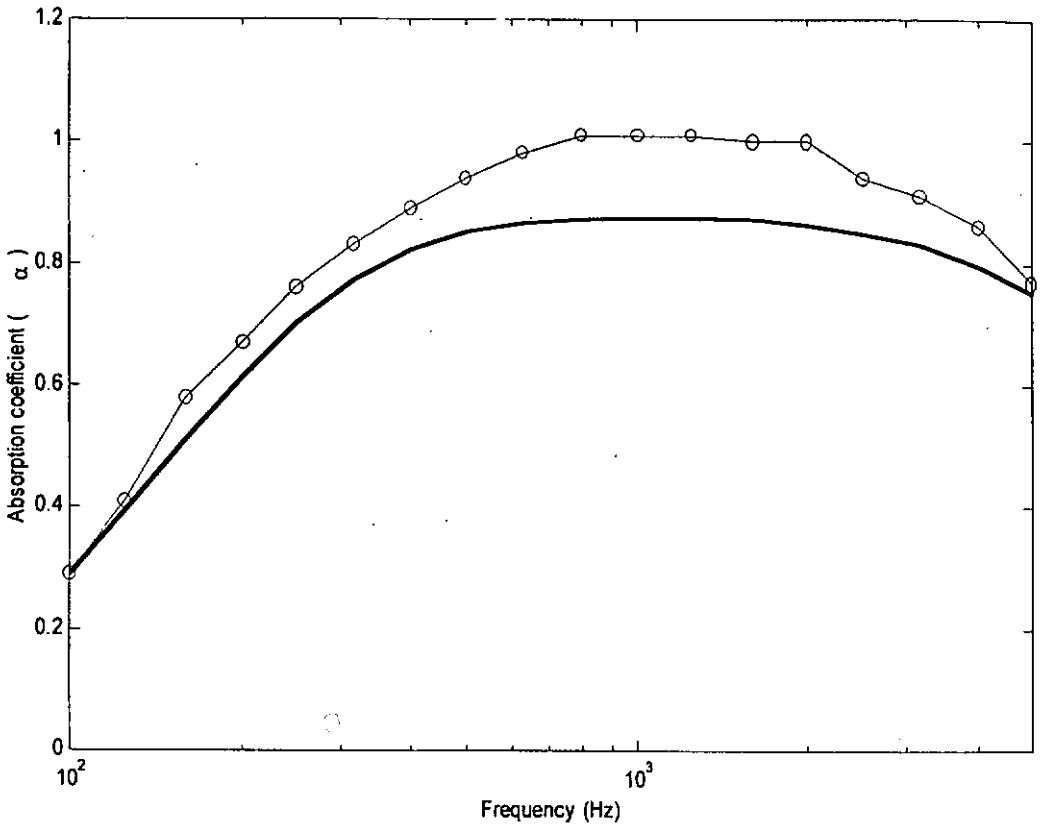

Figure 8 Average Absorption coefficient of perforated facings on sample 1 fiberglass absorber against different frequencies.
Experimental result of average absorption coefficient for random incidence of sound waves (circle line)
Numerical result of average absorption coefficient for random incidence of sound waves (thick solid line)

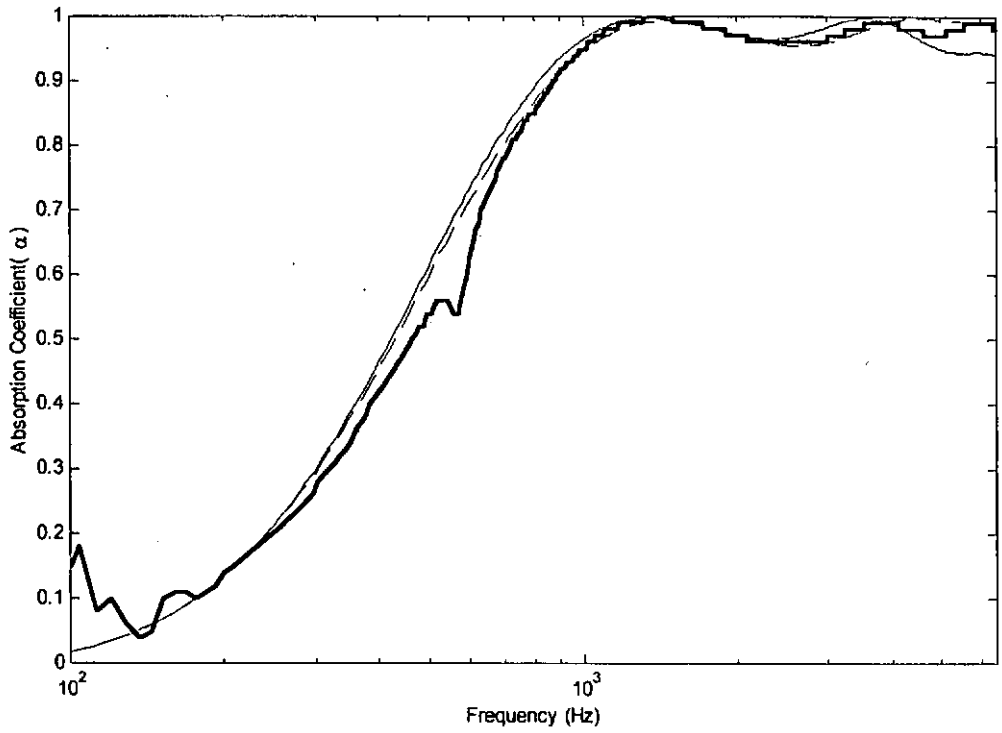

Figure 9 Absorption coefficient of perforated facings on sample 1 fiberglass absorber against different frequencies.
Theoretical result based on proposed theory (solid line), The EECA (dashed line) and Experimental result (thick solid line).

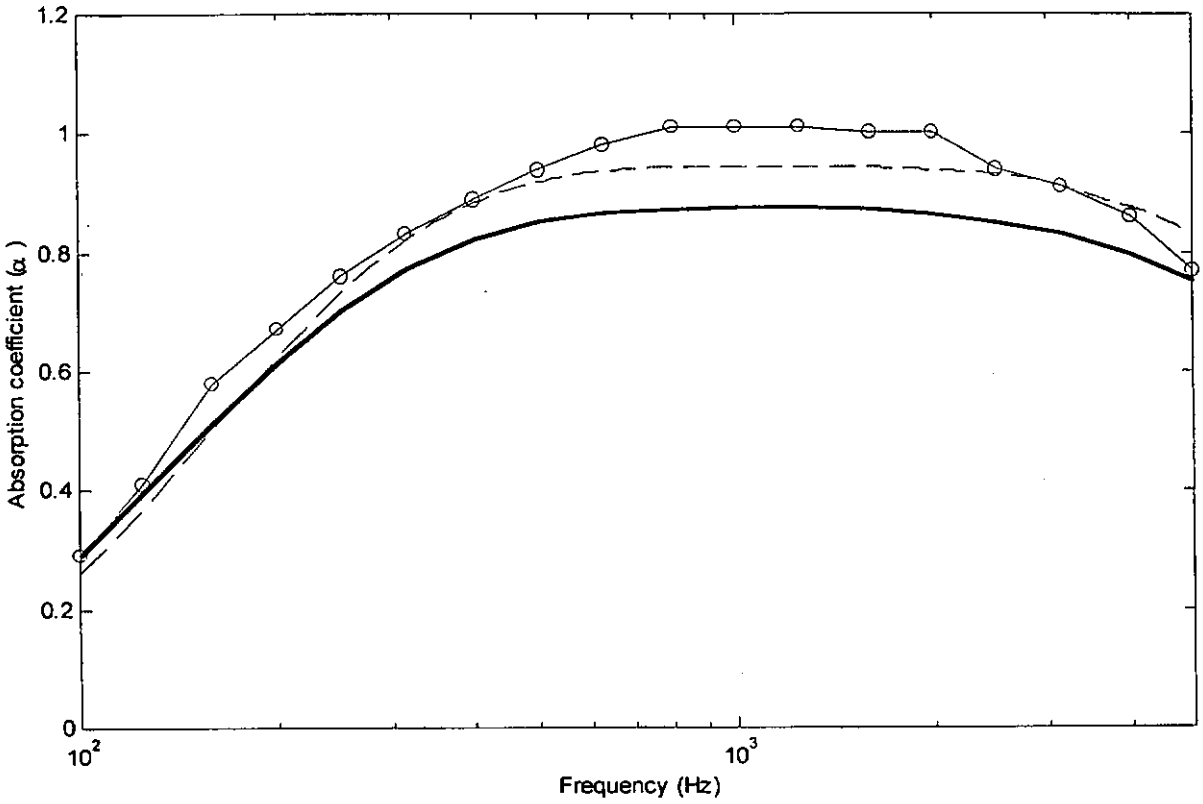

Figure 10 Average Absorption coefficient of perforated facings on sample 1 fiberglass absorber against different frequencies.
Numerical result of average absorption coefficient for random incidence of sound waves (thick solid line), The EECA (dashed line) and Experimental result of average absorption coefficient for random incidence of sound waves (circle)

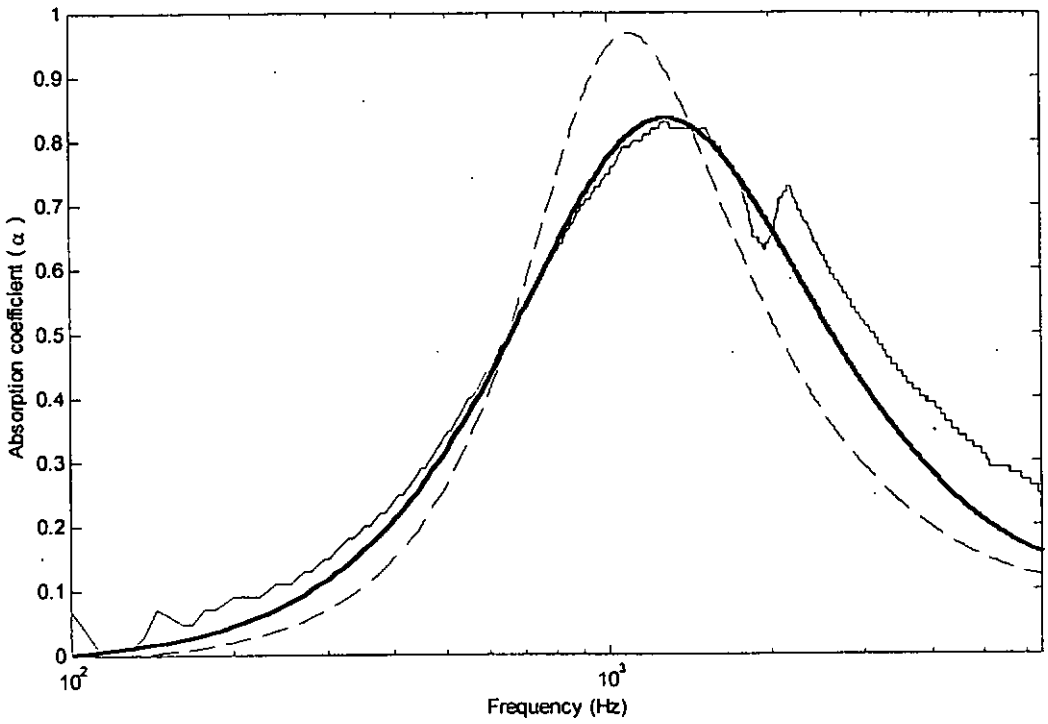

Figure 11 Absorption coefficient of perforated facings with small holes on sample 1 fiberglass absorber against different frequencies.

Parameters: d=2.5mm, b=5mm, t=0.6mm and D_f = 18 mm.

Theoretical result based on proposed theory (thick solid line), The EECA (dashed line) and Experimental result (solid line)

CHAPTER 5

Conclusions

The acoustical characterisation of different types of sound absorbers, such as the fiberglass absorber, the micro-perforated panel (MPP) absorber and the perforated panel (PP) absorber has been determined. A general analytical model has been presented for the evaluation of sound attenuation and absorption coefficient of sound absorbers. Outdoor sound measurement was carried out to determine the sound attenuation above the sound absorbers, the two microphones impedance tube and reverberation room testing method was used to obtain the normal absorption coefficient and average absorption coefficient of the absorbers respectively. The proposed theory shows good agreement with the experimental results.

Chapter 3 briefly reviewed Maa's theory, and then a proposed theory, based on Maa's work and outdoor sound propagation theory, that for the sound absorption performance of the MPP absorber was presented. Such the proposed theory provides detail information of sound absorption of the MPP absorber. It is generally applicable for the study of absorption performance of the MPP absorber in different configurations. This study improves our understanding of the sound absorption performance of MPP absorbers. Moreover, the oblique acoustic impedance of sound waves on the MPP absorber has been validated and the acoustic impedance of mixed construction absorber is presented based on the analytical model. The model shows good agreement with the experimental results for single and double layers of the MPP absorber.

For the perforated panel (PP) covered with fiberglass absorbers, the proposed theory has also given a reasonable agreement with the experimental results. Compared with fiberglass absorbers, the absorption performance of PP absorbers is very similar.

As the resistance of the PP absorbers is low enough, the perforated plate is often used for protection of the fiberglass. For numerical verification of the PP absorbers, boundary element method (BEM), the existing approximate BEM, and 3 dimensional approximate BEM were used to prove the impedance model, which shows a good agreement with the methods, especially the 3 dimensional approximate BEM. Consequently, the proposed theory can provide us with detailed information on the absorption performance of the sound absorbers, the proposed theory has been verified by Equivalent Electrical Circuit Approach (EECA) analysis. In this thesis, a general analytical model is established and allows us to fully understand the acoustical characterisation of the sound absorbers.

APPENDIX: Publication

Law, L.Y. , Li, K.M. and Wong, W.O. "A new analytical model for sound absorption performance of Micro-Perforated Panel Absorber". *Proceedings of Australian Acoustical Society Annual Conference*, Canberra, November 21-23 (2001)

(This paper has been peer reviewed)